Functional redundancy shapes spatial patterns of vulnerability to climate-driven shifts in plant community composition across Australia

Irene Martín-Forés[1,2∓]*, Rhys V. Morgan[3∓], Samuel C. Andrew[4], Rachael V. Gallagher[5], Greg R. Guerin[1]

[1]School of Biological Sciences, The University of Adelaide, Adelaide, South Australia 5005, Australia

[2]TERN – Terrestrial Ecosystem Research Network, The University of Adelaide, Adelaide, Australia

[3]Department for Environment and Water (DEW). South Australian State Government

[4]CSIRO Agriculture & Food, Canberra, Australian Capital Territory, Australia

[5]Hawkesbury Institute for the Environment, Western Sydney University, Richmond, New South Wales, Australia

[∓] These authors contributed similarly.

*Corresponding author: irene.martin@adelaide.edu.au

Abstract

Climate change threatens plant communities worldwide with substantial species losses, yet the consequences of reduced diversity for ecosystem functioning remain uncertain. Functional redundancy, where multiple species fulfil similar ecological roles, may provide functional insurance by buffering ecosystem processes against species loss. Here, we combined plant composition data from 646 TERN AusPlots with gap-filled trait data (maximum plant height, leaf mass per area, and seed dry mass) from the AusTraits database to deliver the first continental-scale assessment of functional redundancy in Australian plant communities.

By explicitly examining diversity metrics and functional redundancy across biomes, we assessed functional vulnerability and buffering capacity under climate change. We estimated potential impacts of species loss under future climates using community thermal and aridity tolerances relative to projected climate exposure. We analysed the continental distribution of functional redundancy (reflecting competitive ability, resource acquisition strategies, and

dispersal–establishment trade-offs), projected climate-driven compositional change, and relationships with bioclimate to identify vulnerable native communities.

Our results revealed strong latitudinal gradients in climate-change impacts, with tropical northern communities facing greater risk of compositional change as future hotter and drier conditions become unsuitable for monsoon-dependent species. Functional redundancy of current vegetation communities increased toward central Australia, aligning with increasingly stressful (hotter, drier) bioclimates. At the biome scale, Mediterranean and arid communities exhibited higher functional redundancy and lower climate risk due to shared drought-adapted traits. Future rainfall changes were the dominant driver of climate-induced shifts in plant community composition.

The most vulnerable communities, at highest risk of functional destabilisation, were located along the northern coastline, with additional hotspots in southern Mediterranean regions of South Australia and Western Australia. Conservation and monitoring efforts should prioritise these regions. Our findings highlight how local bioclimate influences functional redundancy and future climate-change-driven vulnerability, providing a spatial framework to support biodiversity monitoring, policy and land management across Australia.

Keywords: community ecology; climate change; climate risk; ecosystem function; functional traits; functional redundancy; resilience; species loss; vulnerability.

1. Introduction

In the global context of rapid environmental change under widespread threatening processes such as climate change, land use change, and biological invasions (Valladares *et al.* 2019), there is an urgent need to protect biodiversity and better understand its role in the functioning of ecosystems (Díaz *et al.* 2019; Pettorelli *et al.* 2021). By providing a range of functional traits (i.e. measurable attributes or characteristics of species which relate to their fitness and ecological role on ecosystem processes (Gallagher *et al.* 2020)) biodiversity affects ecosystem functioning, productivity, resilience, and stability through complementary and overlapping ecological roles. In this sense, functional redundancy (F_R) quantifies the degree of overlap in functional roles within ecological communities, reflecting the extent to which multiple species contribute similar ecological functions (Walker, 1992). Higher redundancy indicates a greater potential for buffering ecosystem functioning against species loss, as remaining functionally similar species may partially compensate for declines or local extinctions (Walker, 1995). However, such compensation is not guaranteed and depends on whether functionally analogous

species are able to persist and respond positively under changing environmental conditions; if these species are similarly affected by climate stressors, ecosystem functioning may still be impaired despite high redundancy. Importantly, functional redundancy traditionally focuses on species loss, yet climate change can simultaneously drive both species loss and species gain, with incoming species having variable functional consequences ranging from enhanced community resilience to functional disruption.

Consequently, F_R should be interpreted as a measure of potential functional resilience, with low F_R indicating limited capacity to absorb species loss and maintain ecosystem functioning. While Fischer and de Bello (2003) suggested that redundancy implies resilience, with the loss of some species having little detectable effect at the community scale, more recent work has cautioned that this framing may underestimate the unique and context-dependent contributions of species to ecosystem functioning (Eisenhäuer *et al.*, 2023). Here, we retain the F_R framework due to its ecological and conservation relevance in illustrating that certain species can be lost within a community without immediate loss of ecosystem functioning (Fischer and de Bello 2023); however, we acknowledge that it represents one end of a continuum of functional overlap among species, better conceptualised as functional similarity—a spectrum of overlapping but non-identical contributions to ecosystem processes (Eisenhauer *et al.* 2023). Resilience therefore depends not only on the degree of functional overlap, but also on response diversity, defined as variation in how species sharing similar functions respond to environmental change. A limitation of F_R is that functionally similar species may respond in comparable ways to a given stressor, leading to functional loss despite high overlap, such that resilience depends jointly on functional redundancy and response diversity (Elmqvist et al. 2003; Mori et al. 2013).

Functional redundancy is intricately linked to other biodiversity metrics within plant communities, namely species diversity (S_D) and functional diversity (F_D) (Ricotta *et al.* 2016). Species diversity summarises the variety and abundance of taxonomically distinct organisms occurring in ecological communities, whereas F_D summarises the distribution of species and their abundances in the functional trait space of a given community (Mouillot *et al.* 2013). Within a given plant community, the more species that share similar functions (or are redundant in their function), the less vulnerable that function is to loss (Pillar *et al.* 2013). In this sense, species-rich communities (high S_D) often have more species that can perform similar ecological roles, thus increasing the likelihood of functional redundancy (Fonseca and Ganade, 2001). Higher F_D indicates a wide array of ecological functions, being therefore widely considered to reflect overall ecosystem functioning (Cadotte *et al.* 2011). Functional redundancy provides a

more mechanistic link between biodiversity and ecosystem resilience and stability; in the event of S_D loss, higher F_R should buffer a community from losing F_D, as the likelihood of losing a functionally unique species is reduced. In practice, limitations in trait availability and scale often preclude explicit separation of effect traits and response traits, meaning that F_R is commonly interpreted as a proxy for at least some degree of response diversity in large-scale analyses. Such constraints are particularly relevant at continental scales, reinforcing the importance of large-scale open-access trait databases for macroecological assessments of functional resilience (Falster *et al.* 2021).

Despite the growing interest in understanding how F_R affects ecosystem resilience (Biggs *et al.* 2020), how F_R varies at macroecological scales, and the potential drivers of such variation remain understudied. As a result, assessing how functional redundancy varies across climatic gradients and biomes provides a tractable way to link biodiversity structure with potential ecosystem resilience under climate change.

Climate change has driven local and global species extinctions in deep time and is predicted to be a driver of plant extinction in the Anthropocene (Valladares *et al.* 2019). This loss of biodiversity is likely to impair the biological, chemical, and physical processes performed by ecosystems with the specific functional implications of such species loss only beginning to be understood (Hooper *et al.* 2012; Gallagher *et al.* 2013). Climate change, including increasing temperature and changes in precipitation patterns, with subsequent changes in the frequency and duration of drought conditions, are likely to force many plant species beyond their climatic tolerance limits and towards extinction (Lancaster & Humphreys, 2020; Bennett et al. 2021). Assessing the vulnerability of different ecosystems (i.e. the extent to which various ecosystems are likely to be damaged or experience functional disruption) under climate change (e.g. climate-driven stressors such as increasing temperatures and altered precipitation patterns) has become a common practice (Li *et al.* 2018). However, estimates of climate change vulnerability tend to focus on predicted changes to mean climate conditions and the direct impact these will have on species, while ignoring potential resilience mechanisms including individual physiological adaptation/tolerances and community level resilience mechanisms. Gallagher *et al.* (2019) addressed this limitation by measuring the adaptive capacity of Australian vegetation alongside a climate change risk metric (in the sense of projected climate-driven changes in community composition when the environmental niche limits are expected to be surpassed under future climate conditions).

Australia spans one of the widest climatic gradients globally, encompassing tropical, temperate, Mediterranean, and arid ecosystems. This climatic diversity, combined with high

levels of functional variation in plant communities, provides a unique natural laboratory for examining how biodiversity and functionality at the community level will be affected by climate change. We propose that understanding F_R across Australia will also provide complementary information to the impact caused by climate change by indicating the functional resilience of plant communities to species loss. At present, the F_R in Australian plant communities has only been explicitly measured once as part of a global meta-analysis (Laliberté *et al.* 2010). More broadly, continental-scale functional trends and their environmental drivers have seldom been quantitatively investigated in Australian vegetation (Andrew *et al.* 2021, 2025).

Given the potential importance of F_R as an indicator of community resilience to climate change induced species loss, our study seeks to achieve four main aims. These are to (1) determine the geographic distribution of F_R among plant communities across the Australian continent, (2) investigate how F_R varies along bioclimatic gradients, (3) map Australian communities that are most vulnerable to climate change by integrating species' exposure to projected climatic shifts with their sensitivity and adaptive capacity, and (4) examine the relationship between F_R and projected climate driven changes in the composition of sampled plant communities. Specifically, we hypothesised that (1) many locations across Australia would have very low F_D coupled with very high F_R (aligning with a previous study that focused on species-level records across Australia; Andrew *et al.* 2021), due to species niche specialisation driven the continent's diverse and often extreme environmental gradients. Although the direction of the relationship between F_R and bioclimatic variables is unclear in terrestrial plant communities, we expect (2) F_R to be higher in more consistently extreme conditions (*e.g.* increased aridity), where species display drought- and heat-adaptive traits and therefore might be more similar functionally, and overlap more in their strategies evolved as long-term adaptations to persistent environmental stress. Based on well-established climatic gradients across Australia and ecological theory linking global warming exposure and physiological limits to community turnover (di Marco *et al.* 2019), we expect (3) the projected climate driven changes in composition not to be evenly distributed across Australia's plant communities, but reflect instead distinct geographic drivers; specifically, we expect temperature-driven changes to be most acute in the hotter northern regions, and precipitation-driven risks most pronounced in Mediterranean-type ecosystems of southwest Western Australia and southern South Australia. We expect these patterns assuming that many species in these areas may already be close to their thermal or hydric limits (Gallagher *et al.* 2019), and therefore shifts could occur if communities overpass their limit threshold, regardless of their

current F_R. Finally, we expect (4) F_R to be positively associated with projected climate-driven shifts in community composition, particularly in areas expected to become more arid, due to the synergistic effects of increasing heat and drought. Together, these hypotheses are tested using data from the AusPlots ecosystem surveillance network, a standardized, continent-wide vegetation monitoring program designed to capture plant community composition, structure, and functional traits across Australia. This comprehensive standardised field-based dataset allows for a novel biome-specific assessment of how multiple dimensions of biodiversity and functionality mediate climate-change risk at the community scale.

2. Methods

To achieve these aims we combined estimates of F_R with projected climate-driven changes in composition across an existing continental-scale plot network monitoring Australian plant communities. We measured F_R using the three traits of the leaf-height-seed (LHS) scheme which reflects the major axes of plant function: leaf mass per area (LMA), maximum plant height and seed dry mass (Westoby, 1998; Díaz *et al.* 2016). Leaf mass per area (LMA), the inverse of specific leaf area (SLA), captures species' trade-off between carbon investment in leaf-level photosynthetic tissues and leaf longevity (Westoby, 1998; Wright *et al.* 2004). Maximum plant height reflects species' strategies in relation to competition for light and is therefore related to canopy structure and shading in ecosystems (Westoby, 1998; Falster and Westoby, 2003). Seed dry mass indicates species' maternal investment in reproduction and can be related to the capacity to establish across different environmental niches (Westoby, 1998). Afterwards, we measured the climate change risk of individual species based on their observed climatic niches and then scaled this up to the community level by calculating the community weighted mean climate change risk (Gallagher *et al.* 2019), and we mapped F_R and climate change risk to determine their spatial distributions. Finally, we constructed linear regression models to explore the relationship between F_R, climate change risk and environmental variables.

We combined plant community composition data, species functional trait data, long-term climate data, predicted climate change exposure data and species climate niche data to generate our response and predictor variables. The continental approach enables broadscale trends to be detected along key bioclimatic gradients such as temperature and precipitation, elucidating environmental drivers of community-level properties such as F_R and climate change risk (Violle *et al.* 2014). Furthermore, the Australian continental flora is a particularly useful study system due to the contrasting climates existing across the land, that strongly

influence species distribution, and the characteristics of the different ecosystems (Hughes *et al.*, 2003; Keith 2017). Australia is latitudinally characterised by a tropical north with wet summers and dry winters, an arid to semi-arid interior covering most of the continent, and a temperate south with hot dry summers and cool wet winters (Keith 2017). Apart from analysing these trends at the continental scale, to detect scale-dependency in our results we also conducted the analyses at two finer spatial scales. First, we replicated the analyses at the biome scale, using the Ecoregion 2017 dataset based on the classification provided by Olson *et al.* (2001) which designates 7 major biomes in Australia.

2.1. Plant community composition data

The Terrestrial Ecosystem Research Network (TERN) AusPlots ecosystem surveillance program monitors over 1,000 1-ha plots across the Australian continent (Fig. 1) (Sparrow *et al.* 2020). The network is stratified by bioregion to maximise ecological coverage (Guerin *et al.* 2020a) and targets representative vegetation communities that have experienced minimal recent disturbance, based on site selection protocols that avoid areas with recent land-use change, clearing, or intensive management. Within each 1-ha plot, vegetation is surveyed using a standardised point-intercept protocol comprising 1,010 sampling points arranged along ten 100-m transects. At each point, all vascular plant species intercepting a vertical pin are recorded, providing quantitative estimates of species presence and proportional cover that characterise the local plant community (White et al. 2012). These data form the basis for all community-level diversity and functional metrics used in this study. For each plot, a voucher specimen is collected for every recorded species and identified by professional botanists, with determinations lodged in state herbaria, ensuring taxonomic consistency and accuracy. In addition to vegetation composition and structure, AusPlots surveys also record soil properties and landform attributes, including slope (ranging from 0-9° with a median of 1°, and an average of 2.5°) and aspect. These landform variables were not included as predictors in the present analyses because our focus was on broad-scale climatic drivers of diversity and climate-change risk, and because slope and aspect primarily influence local microclimatic variation that is not readily comparable across biomes at the continental scale. Throughout this study, each AusPlots site is treated as a discrete plant community, representing the assemblage of co-occurring species sampled across the full 1-ha area at the time of survey.

We extracted plot-level vascular plant species percent cover data for 787 TERN AusPlots using the 'ausplotsR' package (Guerin *et al.* 2020b; Munroe *et al.* 2021). In cases where repeated surveys were available for plots, the most recent survey was selected to ensure

that the data best reflected current species composition. We used species percent cover data as a proxy for species relative abundances (See supplementary material for the R script for exact extraction workflow).

For analyses at continental-scale we modelled all plots across the TERN AusPlots network together. For biome-scale analyses we grouped plots according to the major biome they occupy in the Olson *et al.* (2001) biome classification (Fig. 1). From analyses at the biome scale, we selected four biomes, including temperate broadleaf and mixed forests (biome 4), tropical/subtropical grasslands, savannas and shrublands (biome 7), Mediterranean forests, woodlands and shrublands (biome 12), and deserts and xeric shrublands (biome 13). Other biomes present in Australia (i.e. biome 1 - Tropical/Subtropical Moist Broadleaf Forests, biome 8 - Temperate Grasslands, Savannas & Shrublands and biome 10 - Montane Grasslands & Shrublands) were excluded from this study due to the low number of TERN AusPlots within their boundaries. These four biomes object of study capture the major climatic and ecological gradients in Australian vegetation. Tropical and subtropical grasslands, savannas, and shrublands (biome 7) are characterized by high mean annual temperatures, strong seasonality in rainfall, and dominance of fire- and drought-adapted species, often occupying narrow ecological niches (Shaw *et al.* 2000). Temperate broadleaf and mixed forests (biome 4), in contrast, experience moderate temperatures and relatively stable precipitation, supporting higher species richness and less extreme functional constraints (Bailey, 1964). Mediterranean forests, woodlands, and shrublands (biome 12) in southwestern and southeastern Australia are shaped by hot, dry summers and mild, wet winters, favouring species with stress-tolerant or drought-avoidance strategies (Lionello *et al.* 2006). Deserts and xeric shrublands (biome 13) are characterized by extremely low precipitation, high temperatures, and high climatic variability, resulting in plant communities strongly constrained by environmental filtering (Noy-Meir, 1973). Grouping plots by these biomes allows us to assess context-specific functional responses, capturing how climate, species physiology, and evolutionary history interact to shape diversity and functional redundancy across contrasting environmental settings (Laliberté *et al.* 2010).

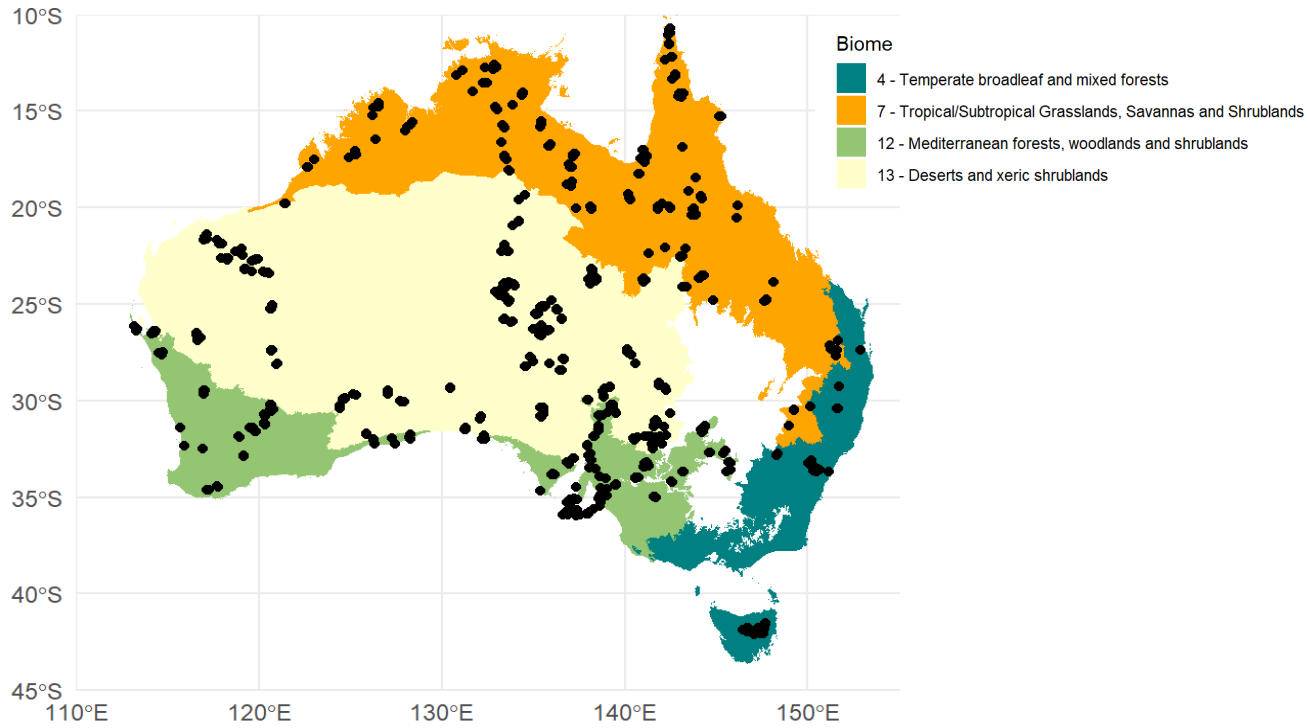

Figure 1. Biomes of Australia used in this study and geographic locations of AusPlots flora inventories (black circles). Biome 4 – Temperate broadleaf and mixed forests (n = 43 plots), biome 7 – Tropical/Subtropical Grasslands, Savannas & Shrublands (n = 218 plots), biome 12 - Mediterranean Forests, Woodlands & Shrublands (n = 203 plots), biome 13 - Deserts & Xeric Shrublands (n = 280 plots). Note that several biomes were excluded from this study due to the low number of TERN AusPlots within their boundaries: biome 1 - Tropical/Subtropical Moist Broadleaf Forests (n = 0), biome 8 - Temperate Grasslands, Savannas & Shrublands (n = 28) and biome 10 - Montane Grasslands & Shrublands (n = 15).

2.2. Trait data

We extracted trait data from the AusTraits database 6.0.0 for all species occurring in our plots. AusTraits contains data for 448 functional traits across 28,640 Australian taxa compiled from multiple sources (Falster *et al.* 2021).

From the 4,428 species recorded in AusPlots with the point intercept methodology, we obtained mean values for maximum plant height (3,641 species), leaf mass per area (LMA) (1,304 species), and seed dry mass (2,574 species), respectively. We log transformed all trait values to account for differences in their units and skewness in their distributions, which is standard for community trait analysis (Bruelheide *et al.* 2018). To improve species representation, we followed the methods outlined in Andrew *et al.* (2021), consisting of two

subsequent steps by which missing trait values were first estimated missing values via linear models, and subsequently gap-filled utilising all accessible and relevant trait data from the native Australian flora. In summary, to leverage the available measurements of leaf/phyllode and seed dimensions for a significant proportion of species in AusTraits, we first estimated leaf area for species lacking direct area measurements based on measurements of leaf length and width. To do so, we conducted Linear Mixed Models (LMM) using the lme4 R package (Bates 2010). Likewise, seed dry mass was estimated using seed length as a fixed effect, combined with a random factor of family. Predicted trait values were well correlated to known values (seed mass $r^2 = 0.85$, leaf area $r^2 = 0.81$). The models demonstrated strong explanatory power, evidenced by high conditional R^2 values (R^2_c) for both trait models, with a substantial portion of the explanatory power derived from fixed effects, reflected in high marginal R^2 values (seed dry mass: $R^2_c = 0.85$; $R^2_m = 0.68$; leaf area: $R^2_c = 0.79$; $R^2_m = 0.66$).

We adopted a minimum threshold of 80% trait coverage by abundance for plots to be included in our study as this threshold has been shown to limit the estimation bias of community weighted functional properties (Borgy *et al.* 2017). In a second step, to increase the taxonomic coverage of trait data we gap-filled values for species without direct observations in AusTraits using the GapFilling() function from the BHPMF R package (Schrodt *et al.*, 2015), which employs Bayesian hierarchical probabilistic matrix factorisation and correlation structure to impute missing trait values. This method exploits trait–trait correlations and phylogenetic trait signals within the existing trait data to predict unknown trait values. Gap-filling was run on a matrix of trait values for plant height, leaf area, length, and width, leaf mass per area (inverse of SLA), and seed mass and length; species with no available trait data were dropped from all subsequent analyses (n = 24,915 native Australian plant species retained). Finally, we applied the 80% trait coverage by abundance threshold to the total of 787 AusPlots, leaving 649 plots which met the threshold.

2.3. Diversity indices

We calculated four diversity indices, including species richness (S_R), species diversity (S_D), functional diversity (F_D) and functional redundancy (F_R). We followed the methodology of Ricotta *et al.* (2016) in which S_D is calculated as Simpson's diversity index and F_D is calculated as Rao's quadratic entropy. Simpson's diversity is bound between 0 and 1 and it incorporates plot-level species relative abundances. Rao's quadratic entropy is also bound between 0 and 1 and it accounts for plot-level species relative abundances as well as species pairwise functional dissimilarities. Rao's quadratic entropy is ultimately the mean functional dissimilarity of two

randomly selected individuals from a given community (Botta-Dukát, 2005). Importantly, the maximum value of Rao's, when all species are maximally functionally dissimilar, is equal to Simpson's index. Therefore, dividing S_D by F_D yields a measure of the functional uniqueness of a community (U).

$$U = \frac{F_D}{S_D} \qquad \text{(eq. 1)}$$

The complement of U is a measure of the functional redundancy of a community (F_R), which summarises the proportion of species diversity not encompassed by functional diversity.

$$F_R = 1 - U \qquad \text{(eq. 2)}$$

All alpha diversity indices were computed with the 'uniqueness' R function provided by Ricotta *et al.* (2016).

To assess whether F_R exhibited any statistically detectable geographic structure, we quantified spatial autocorrelation using Moran's I with a 5-nearest-neighbour spatial weights matrix. In addition, we evaluated broad spatial trends by modelling F_R as a function of latitude and longitude (second-order polynomial terms). To assess whether F_R differs among major Australian biomes, we also conducted a one-way ANOVA with subsequent Tukey HSD post-hoc tests to evaluate pairwise differences among biomes.

Finally, we also calculated the F_D–F_R ratio, as an indicator between different community properties, namely functional breadth (represented by F_D) relative to functional overlap (F_R). The F_D–F_R ratio provides an integrated perspective on whether communities are dominated by many distinct strategies or by multiple species sharing similar traits.

2.4. Bioclimatic data

We obtained long term (1970-2000) mean climate data in a raster format from 'WorldClim 2.1' and extracted values at the coordinates of each plot (Fick and Hijmans, 2017) at a resolution of 10 minutes of a degree. We extracted mean annual temperature (MAT; °C), temperature annual range (T-Range; °C), maximum temperature of the warmest month (T-Max; °C), mean annual precipitation (MAP; mm), precipitation seasonality (P-Seasonality) and precipitation of the driest month (P-Dry; mm). These variables reflect the mean, variability, and extremes of temperature and precipitation, all of which are projected to change under future climate scenarios for Australian ecosystems (Hughes, 2003).

2.5. Future climate projections and climate change risk

To assess the climate change risk faced by plant communities across Australia, we followed an approach informed by Gallagher *et al.* (2019), by adapting their grid-based methodology in order to calculate plot-based climate change risk metrics. We calculated metrics of risk for changes to both MAT and MAP. For these calculations we used the same set of species as in the diversity index calculations to enhance comparability between diversity indices and climate change risk metrics. First, we obtained species-level climate niche data compiled by Gallagher *et al.* (2019), which represents the realised climatic limits of Australian plant species based on cleaned occurrence records for herbarium specimens from the Australian Virtual Herbarium (AVH). To account for potential outliers in these occurrence records, we defined species' temperature tolerance (MAT tolerance) as the 98th percentile of mean annual temperature (MAT) values across their distribution, and precipitation tolerance (MAP tolerance) as the 2nd percentile of mean annual precipitation (MAP) values. We then matched these species-level climate tolerances to the species occurring in each plot and calculated community-weighted mean (CWM) climate tolerances by multiplying each species' tolerance value by its relative abundance in the plot. These CWMs represent the average climatic tolerance of the plant community in terms of upper temperature and lower precipitation limits.

To assess current climatic safety margins, we subtracted the present-day (baseline) climate conditions from the community-weighted mean tolerance values at each plot. Specifically, for MAT and MAP, the safety margins were, respectively, calculated as:

$$MAT\ Safety\ Margin = CWM\ MAT\ Tolerance - Current\ MAT$$

$$MAP\ Safety\ Margin = Current\ MAP - CWM\ MAP\ Tolerance$$

These safety margins represent the climatic buffer a plant community has before it reaches its collective thermal or drought limit.

Australia is projected to experience substantial warming by 2070, with mean annual temperatures expected to increase across the continent, particularly in the interior and northern regions. Precipitation patterns are likely to become more variable, with decreases in cool-season rainfall and longer drought duration projected for many parts of the south and east (especially mediterranean-type regions), while some northern areas may experience more intense wet-season rainfall events (State of the Climate 2024). Hence, we then estimated future climate exposure by calculating projected changes in MAT and MAP between current climate conditions and predicted projections for 2070 under the high-emissions scenario RCP8.5 (rcp85, 800 ppm of CO_2 by 2070). For that, we used downscaled climate data from CHELSA

based on five global circulation models for 2061-2080, including ACCESS1.0, CNRM-CM5, HADGEM2-CC, MIROC5, and NorESM1-M.

Finally, we calculated plot-level climate change risk as the difference between exposure and safety margin:

$$MAT\ Risk = Exposure - Safety\ Margin$$

$$MAP\ Risk = -(Exposure - Safety\ Margin)$$

For MAT, a positive risk value indicates that future climate change by 2070 in terms of temperature is expected to exceed the current adaptive capacity of the community (i.e. the community's mean tolerance limit), placing it at greater risk. Conversely, negative or low risk values suggest that the community's climatic buffer is sufficient to accommodate projected temperature changes. For MAP, the opposite, when Exposure − Safety Margin has a negative value indicates that future drought conditions by 2070 are expected to exceed the current adaptive capacity of the community, placing it at greater risk, whereas positive values suggest that the community's climatic buffer is sufficient to accommodate projected temperature changes, hence why the values have been multiplied by (-1).

We acknowledge that species respond individually to climate change and that communities are not strictly discrete units. Community-weighted mean (CWM) tolerances provide an operational estimate of the average climatic tolerance of the dominant species in each plot, capturing the functional response of the community as a unit. While individual species may exceed their limits without immediately altering functional diversity, CWM-based safety margins allow community-level comparison of climate change risk across a given spatial scale.

2.6. Mapping alpha functional redundancy and climate change risk

To visualise the spatial distribution of F_R and climate change risk we created maps depicting their values across the TERN AusPlots continental network using the ggplot2 (Wickham 2016) and ggpmisc (Aphalo 2025) packages in R. We generated separate maps for MAT Risk, MAP Risk and alpha F_R. Additionally, we constructed bivariate maps –derived directly from quantitative, plot-level metrics, ensuring that observed patterns reflect measured differences rather than subjective interpretation– which illustrates F_R and climate change risk simultaneously for each plot. For mapping functional redundancy (F_R) and climate change risk (MAT and MAP), we classified plots into three categories each. F_R categories were defined as follows: low redundancy corresponded to the lowest 33% of F_R values, medium redundancy

included values between the 33rd percentile and the 67th percentile of plots considered at risk, and high redundancy included values above the 67th percentile. This approach aims to emphasize relative differences in buffering capacity among communities, rather than assuming an absolute redundancy threshold, and to highlight areas that have considerably lower functional redundancy than others and therefore are subjected to higher risk under climate change. Climate-change risk categories were defined using biologically meaningful thresholds; MAT Risk was classified as low risk for plots that were not at risk (MAT Risk < 0); similarly, MAP Risk was classified as low risk for plots that were not at risk (MAP Risk > 0). Among plots at risk (MAT Risk ≥ 0 and MAP Risk ≤ 0), we then used the median of the at-risk subset to distinguish medium and high risk categories. approach ensures that the classification reflects both the distribution of F_R and the degree of climate change exposure among at-risk plots, avoiding the bias introduced by equal-interval or quartile-based splits of the entire dataset. These classifications were used exclusively for visual synthesis in bivariate maps and do not affect statistical analyses. Together, they facilitate the identification of relative vulnerability hotspots (high climate-change risk combined with low F_R) and support spatial comparison across regions while preserving the underlying quantitative nature of the data. Beyond serving as a visual illustration, these bivariate maps provide an analytical framework to identify spatial patterns and hotspots of vulnerability, (high climate change risk and low F_R), highlighting plots that will likely undergo climate-driven changes in community composition and enabling comparison across regions and prioritisation for conservation or further study.

2.7. Modelling the relationship between diversity indices, bioclimate and climate change risk

We investigated the drivers of plant diversity metrics (species richness, S_R; species diversity, S_D; functional diversity, F_D; functional redundancy, F_R) and climate-driven vulnerability (MAT Risk, MAP Risk) using linear regression models at two spatial scales: continental (all AusPlots across Australia) and biome-specific. For diversity metrics, we included six bioclimatic predictors (MAT, T-Max, T-Range, MAP, P-Dry and P-Season). For climate risk metrics, we tested two complementary predictor sets: bioclimatic variables and diversity indices (S_R, S_D, F_D, F_R). All models were additive and excluded interactions. We evaluated all possible models containing any subset of predictors, including the null model, and selected the best-supported model based on the lowest Akaike Information Criterion (AIC). For each model, we calculated ΔAIC and Akaike weights, with ΔAIC < 2 indicating substantial support. From each best-supported model, we extracted slopes, standard errors, t-values, p-values, and goodness-of-fit

metrics (R^2, adjusted R^2, residual standard error, AIC, BIC) to quantify the strength, direction, and significance of predictors. Only results from the best-supported models are reported.

3. Results

Species richness (S_R) averaged 21.01 species per plot (± 11.17 Standard Deviation (SD); Inter Quartile Range (IQR) = 13–27) , indicating high variability across the sampled sites. Species diversity (S_D) had a mean of 0.72 (± 0.18 SD; IQR = 0.64–0.85), while quadratic functional diversity (F_D) averaged 0.18 (± 0.07 SD; IQR = 0.14–0.22). Functional redundancy (F_R) in sampled plant communities ranged from 0.44 to 0.93, with a mean value of 0.75 (± 0.07 SD; IQR = 0.71–0.80).

While no dominant spatial gradient in F_R was evident across the continent (Fig. 2), F_R exhibited weak but significant positive spatial autocorrelation (Moran's I = 0.205, $p \leq 0.001$), indicating that nearby plots tend to be more similar in F_R than expected by chance. A spatial model including second-order polynomial terms for latitude and longitude detected statistically significant non-linear spatial structure; however, spatial position explained only a small proportion of the overall variation in F_R (polynomial model: adjusted $R^2 = 0.048$, $p < 0.001$). This indicates that, although broad and non-linear geographic patterns exist (including a tendency for higher F_R in interior regions), spatial location is a relatively minor contributor to continental-scale variation in F_R, consistent with our interpretation of weak geographic gradients rather than strong spatial control. As such, central Queensland, the arid zones of South Australia and the Northern Territory, and parts of western New South Wales appeared as hotspots of high F_R. In contrast, regions such as Tasmania, eastern New South Wales, the west coast of Western Australia, the northern tip of the Northern Territory, and the Mount Lofty Ranges in South Australia exhibited mostly lower F_R values. When comparing F_R across biomes, we found significant differences (ANOVA: $F = 10.42$, $p \leq 0.001$). Pairwise comparisons (Tukey HSD) indicate that some biomes, including the arid deserts and xeric shrublands (biome 13) and the tropical and subtropical grasslands, savannas and shrublands (biome 7), had significantly higher F_R than Mediterranean-type (biome 12) and temperate forest (biome 4) biomes (see supplementary material for further details). Overall, plots with high F_R were not strongly spatially segregated from those with low F_R; thus, despite these broad-scale differences, high and low F_R plots remain intermixed locally, supporting our original conclusion that fine-scale hotspots (e.g., Central Queensland, Mount Lofty Ranges) reflect site-level variation that cannot be fully captured by biome aggregation. We note, however, that some of this local variability may also reflect the necessarily sparse sampling of large-scale

ecosystems by 1-ha plots, such that fine-scale heterogeneity within landscapes can contribute to apparent spatial variability in F_R at continental scales.

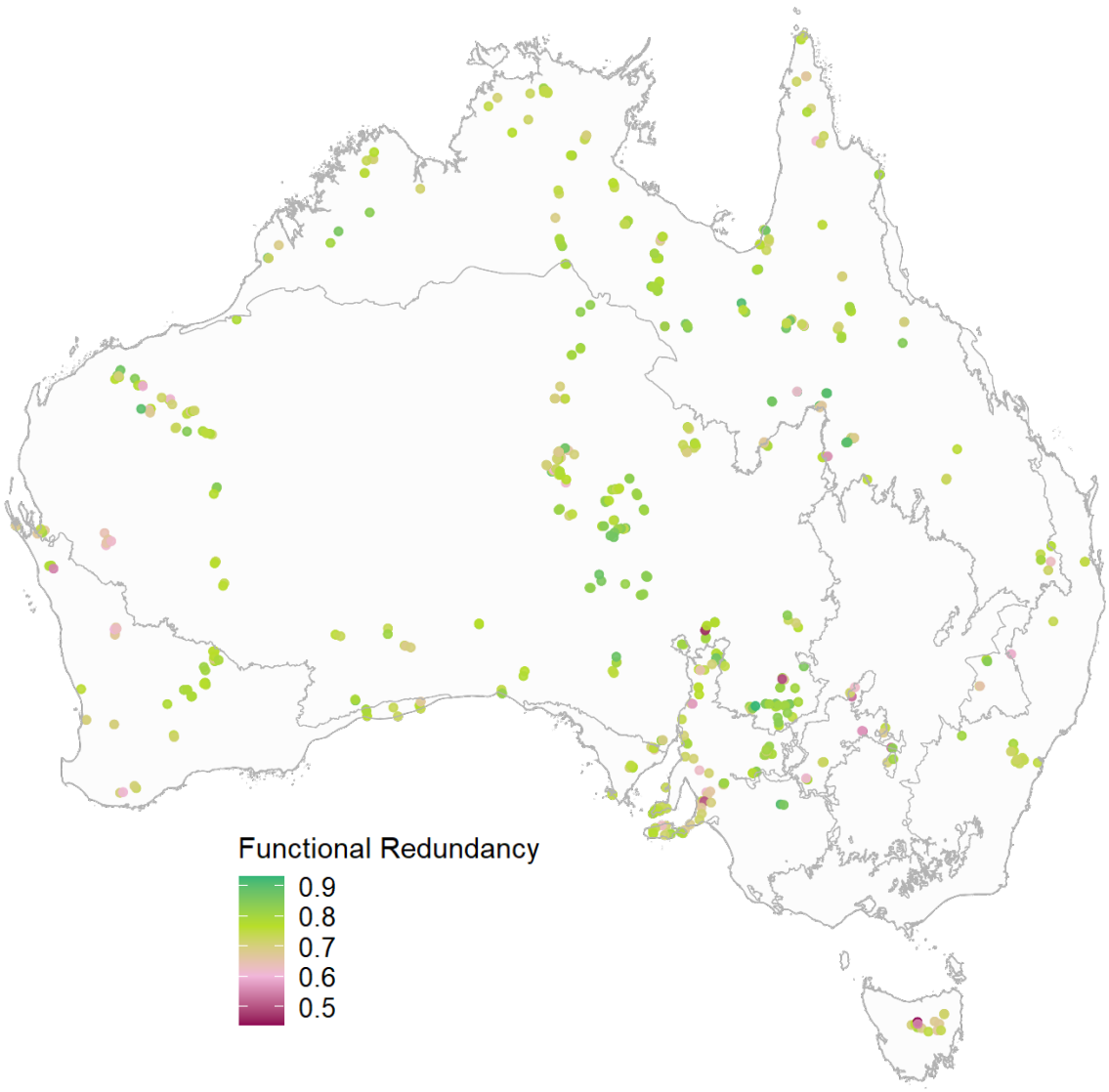

Figure 2. Map of plot-level functional redundancy values across the TERN continental vegetation monitoring plot network (n = 646; notice that for three plots, calculations of certain diversity metrics were not possible). Colour denotes functional redundancy values at each plot (legend). Black lines indicate the approximate boundaries of major Australian biomes, shown for geographic context.

3.1. Variation of diversity indices along bioclimatic gradients

While some temperature variables were correlated (e.g., MAT and T-Max, $r = 0.87$, $p \leq 0.001$; see supplementary material for further details), we show their independent bivariate relationships to illustrate the different ecological dimensions of each bioclimatic variable.

Across Australia, multivariate AIC-selected models revealed consistent climatic influences on plant diversity patterns. Species richness and diversity (S_R and S_D), and functional diversity (F_D) were primarily shaped by temperature–precipitation trade-offs, with temperature predictors exerting predominantly negative effects and mean annual temperature showing mainly positive associations (see Table 1 for specific significant effects). Together, these models explained between 7% and 24% of the variation in S_R, S_D, and F_D. In contrast, functional redundancy (F_R) responded only weakly to climate, increasing with mean temperature and thermal range and decreasing with maximum temperature and precipitation seasonality. Although several predictors were retained in the best model for F_R, this only explained 4% of its variation, indicating that functional redundancy seems to be decoupled from broad-scale climatic gradients.

Biome-level analyses revealed marked regional differentiation in the climatic drivers of plant diversity (see Table 2 for specific significant effects; Supplementary material). In temperate broadleaf and mixed forests (biome 4), diversity patterns were mainly structured by temperature variability, with species richness and functional diversity declining under greater thermal range, while precipitation variables played a stronger role in shaping species diversity. In tropical savannas (biome 7) pulsed water availability displayed a central role, species richness increased with mean temperature but declined under higher thermal extremes and stronger precipitation seasonality, species and functional diversity were positively associated with annual precipitation and negatively by increasing rainfall seasonality, whereas functional redundancy was positively influenced by thermal range. In Mediterranean forests, woodlands and shrublands (biome 12), precipitation was the dominant driver, with richness, species diversity and functional diversity increasing with stronger seasonal and dry-period rainfall, alongside negative effects of mean temperature; functional redundancy in this biome declined with increasing thermal and hydric stress. In deserts and xeric shrublands (biome 13), species richness and functional diversity responded to contrasting temperature and precipitation gradients, and functional redundancy declined under greater climatic variability. Together, these biome-specific patterns indicate that plant diversity metrics respond to distinct climatic constraints depending on regional environmental context.

Table 1. Best-fit linear models explaining spatial variation in species richness (SR), species diversity (SD), functional diversity (FD), and functional redundancy (FR) across Australia and within selected biomes. Models were selected using AIC-based stepwise selection. The table reports the retained predictors, model fit statistics (adjusted R^2, sigma), and Akaike Information Criterion (AIC). The direction and statistical significance of each predictor in the best model are shown in brackets after each term (+: positive effect; –: negative effect; * $p \leq 0.05$, ** $p \leq 0.01$, *** $p \leq 0.001$). Predictors without brackets were retained in the best model but were not statistically significant.

Response Variable	Best model formula	Adj R^2	sigma	AIC	$df_{residual}$
S_R	SR ~ MAT$^{(-***)}$ + T_Max $^{(+***)}$ + T_Range$^{(-***)}$ + MAP$^{(+***)}$ + P_Season$^{(+*)}$	0.23	9.75	4783.56	640
S_D	SD ~ MAT$^{(-***)}$ + MAP$^{(+***)}$ + P_Dry$^{(-***)}$	0.07	0.08	-434.38	642
F_D	FD ~ MAT$^{(-***)}$ + T_Max $^{(+*)}$ + T_Range + MAP$^{(+***)}$ + P_Dry$^{(-**)}$	0.11	0.11	-1764.83	640
F_R	FR ~ MAT$^{(+***)}$ + T_Max$^{(-**)}$ + T_Range$^{(+**)}$ + MAP + P_Season$^{(-*)}$	0.04	0.04	-1566.12	640
Biome 4 – Temperate broadleaf and mixed forests					
S_R	SR ~ T_Max$^{(+***)}$ + T_Range$^{(-***)}$	0.54	8.30	231.10	29
S_D	SD ~ MAT + MAP$^{(+**)}$ + P_Dry$^{(-*)}$ + P_Season$^{(-*)}$	0.21	0.16	-18.81	27
F_D	FD ~ T_Range$^{(-*)}$	0.14	0.06	-84.79	30
F_R	FR ~ MAT	0.03	0.07	-72.10	30
Biome 7 – Tropical / subtropical grasslands, savannas and shrublands					
S_R	SR ~ MAT$^{(+***)}$ + T_Max$^{(-***)}$ + P_Dry$^{(-**)}$ + P_Season$^{(-***)}$	0.29	9.91	1291.47	168
S_D	SD ~ MAT + MAP$^{(+***)}$ + P_Season$^{(-*)}$	0.12	0.17	-114.92	169
F_D	FD ~ MAP$^{(+***)}$ + P_Season$^{(-*)}$	0.13	0.06	-473.37	170
F_R	FR ~ T_Range$^{(+*)}$	0.03	0.07	-431.87	171
Biome 12 – Mediterranean forests, woodlands and shrublands					
S_R	SR ~ MAT$^{(-***)}$ + T_Max$^{(+**)}$ + P_Dry$^{(+***)}$ + P_Season$^{(+*)}$	0.48	8.30	1201.84	164
S_D	SD ~ MAT$^{(-**)}$ + P_Season$^{(+***)}$	0.16	0.15	-165.96	166
F_D	FD ~ P_Dry$^{(+***)}$ + P_Season$^{(+***)}$	0.21	0.06	-489.30	166
F_R	FR ~ MAT$^{(-***)}$ + MAP$^{(-***)}$ + P_Dry$^{(-***)}$	0.18	0.07	-433.99	165
Biome 13 – Deserts and xeric shrublands					

S_R	$SR \sim MAT^{(-***)} + T\_Max^{(+**)} + T\_Range^{(-*)} + MAP^{(+***)}$	0.09	8.25	1658.41	229
S_D	$SD \sim P\_Season^{(+*)}$	0.01	0.17	-161.00	232
F_D	$FD \sim MAT^{(-***)} + T\_Max^{(+***)} + MAP + P\_Season^{(+*)}$	0.06	0.06	-653.69	229
F_R	$FR \sim MAT^{(+***)} + T\_Range^{(-***)} + MAP^{(-*)} + P\_Season^{(-**)}$	0.13	0.07	-605.50	229

529

3.2. Geographic distribution of climate change risk and its relationship to environmental variables

Out of 649 plots, 201 (31%) are considered at risk to species turnover and changes in community composition due to projected changes in mean annual temperature (Risk MAT ≥ 0; Fig. 3). Plots with the highest Risk MAT values are primarily located in the northern half of the continent, whereas lower-risk plots occur at more southerly latitudes. Meanwhile, 608 plots (93.7%) are considered at risk from predicted changes in mean annual precipitation (Risk MAP ≤ 0), with the highest-risk plots generally located at the northern and southern extremes of the continent and lower-risk plots in central regions (Fig. 3). Across the TERN AusPlots network, regression analyses revealed that Risk MAT increases strongly with latitude ($R^2 = 0.58$, $p < 0.001$), indicating higher temperature-driven risk in northern regions (slope = 0.254 °C per decimal degree latitude; Fig. 4). Incorporating longitude slightly improved model fit ($R^2 = 0.66$, $p < 0.001$), showing that risk rises northwards but decreases slightly westwards (longitude slope = -0.071 °C per decimal degree). In contrast, Risk MAP declines with latitude ($R^2 = 0.20$, $p < 0.001$), suggesting greater precipitation-driven risk in southern regions. These regression models complement the histograms and maps, quantitatively highlighting broad latitudinal trends in climate change exposure.

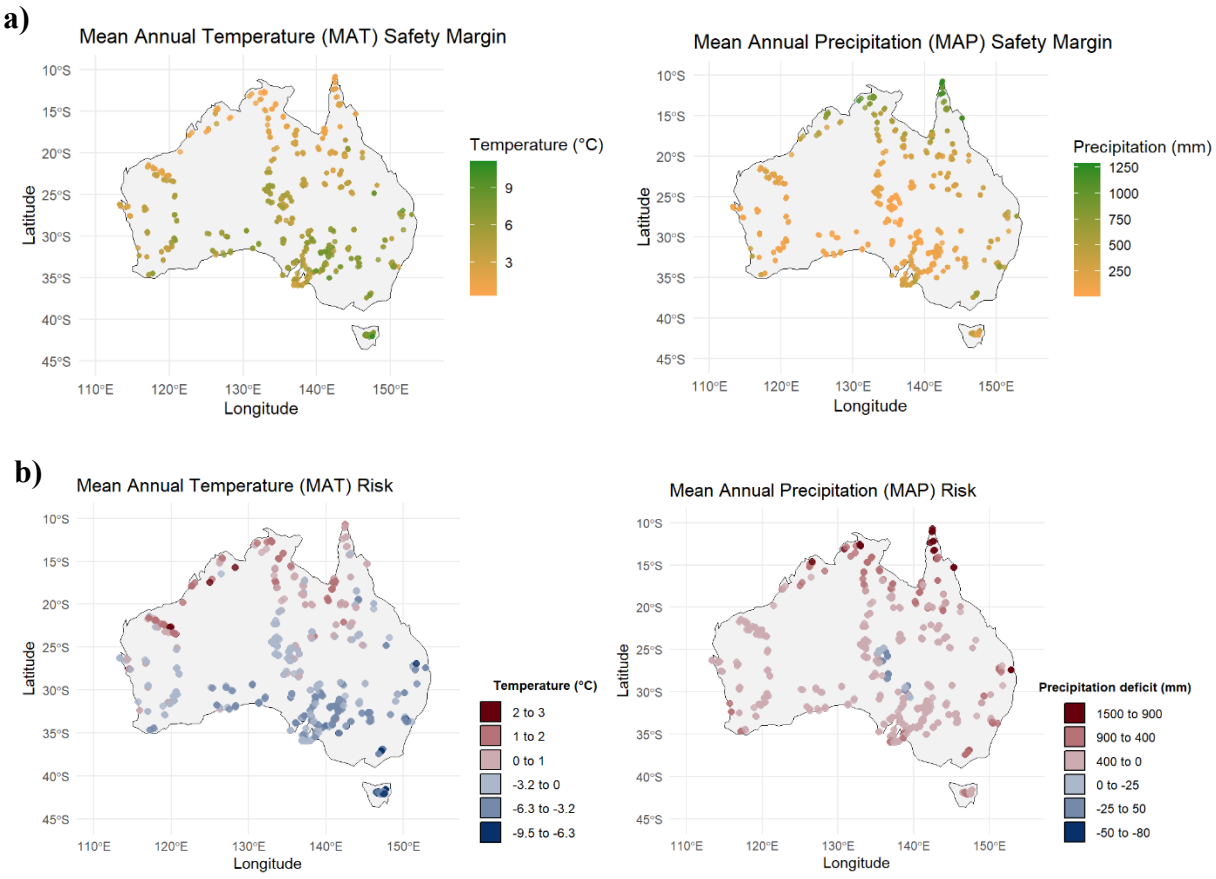

Figure 3. a) mean annual temperature (MAT) (left) and mean annual precipitation (MAP) (right) safety margins; **b)** climate change risk in terms of predicted changes to MAT (left) and MAP (right) across the TERN AuPlots network; **c)** distribution histograms of Risk MAT and Risk MAP. For MAT climate change risk, notice that the values in the legend represent °C, over (positive) or below (negative) the safety margin, to which the vegetation community will be exposed in the future. For MAP climate change risk, notice that the values in the legend represent water deficit, over (positive; i.e. more water deficit and harsher conditions) or below (negative) the safety margin, to which the vegetation community will be exposed in the future. Red points on the map represent at risk plots, while blue colours represent plots with risk values of zero or less (the darker the blue the less at risk).

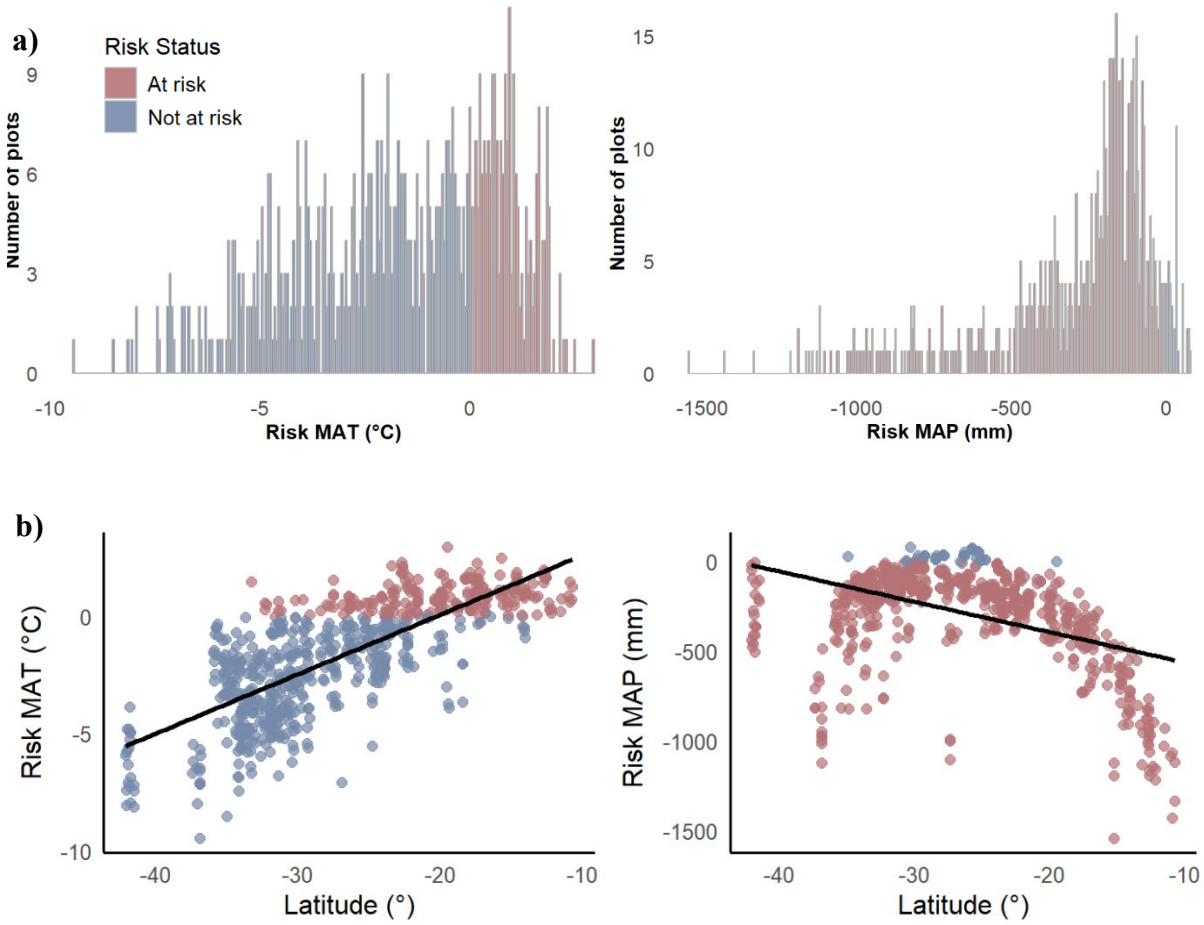

Figure 4. a) distribution histograms of Risk MAT and Risk MAP; and **b)** scatterplots of Risk MAT and Risk MAP versus latitude with fitted linear regression lines (solid), illustrating broad latitudinal trends in climate change exposure across the network. On both the histograms and the scatterplots, red represents plots at risk (positive for MAT, negative for MAP), while plots not at risk are shown in blue, highlighting the big proportion of plots at risk across the network.

Across all AusPlots, MAT Risk increased with higher T-max and P-season, and decreased with increasing MAT and temperature range (T-Range), indicating that sites in hotter regions with marked precipitation seasonality are projected to experience greater temperature-driven turnover (Table 2; see supplementary material for full model outputs). In contrast, MAP Risk increased with MAT, MAP, P-dry, and P-season, and decreased with T-range and T-max, suggesting that precipitation-driven turnover is highest in warm sites with moderate temperature variability (Table 2; Supplementary material). MAP Risk displayed an inverse pattern, increasing with MAT and T-Range and decreasing with MAP and T-Max, with an additional negative effect of P-Dry. These patterns indicate that temperature-driven and precipitation-driven turnover risks respond to distinct climatic axes, with the former most

elevated in warmer and seasonal environments, and the latter being greater in hotter and arid regions.

Biome-level analyses revealed marked regional differentiation in the climatic drivers of plant diversity (Table 2; Supplementary material). In temperate broadleaf and mixed forests (biome 4), diversity patterns were primarily structured by temperature extremes, with species richness increasing with maximum temperature and declining with temperature range, and functional diversity also decreasing with greater thermal variability. By contrast, species diversity in this biome was more strongly associated with precipitation, increasing with mean annual precipitation and declining with both dry-season rainfall and precipitation seasonality. In tropical and subtropical grasslands, savannas and shrublands (biome 7), temperature and precipitation exerted opposing influences: species richness increased with mean annual temperature but declined with maximum temperature and indicators of dry or seasonal rainfall, while species diversity and functional diversity were most strongly and positively associated with mean annual precipitation and negatively affected by precipitation seasonality. Functional redundancy in this biome showed a weak but positive association with temperature range. Mediterranean forests, woodlands and shrublands (biome 12) were dominated by precipitation effects, with species richness, species diversity and functional diversity all positively related to dry-season rainfall and precipitation seasonality, alongside negative effects of mean annual temperature on richness and diversity. Functional redundancy in this biome declined with increasing temperature and precipitation, indicating sensitivity to both thermal and hydric stress. In deserts and xeric shrublands (biome 13), species richness declined with mean annual temperature and temperature range but increased with maximum temperature and mean annual precipitation. Species diversity increased with precipitation seasonality, while functional diversity declined with mean annual temperature and increased with maximum temperature and precipitation seasonality. Functional redundancy in this biome increased with temperature but declined with thermal variability and precipitation.

3.3. Relationship between climate change risk and diversity metrics

At the continental scale, MAT Risk was not significantly related to any of the diversity metrics examined (species richness, species diversity, functional diversity, or functional redundancy). In contrast, MAP Risk was significantly related to all metrics; specifically, species richness, species diversity, and functional diversity all showed significant positive relationships with MAP Risk, indicating that sites with higher diversity tends to occur in areas projected to experience greater precipitation-related risk. In contrast, functional redundancy was negatively

related to MAP Risk, suggesting that lower redundancy is associated with higher precipitation-related risk (Table 3).

At the biome scale, correlations varied among biomes. The only significant relationships found for MAT Risk were in Mediterranean systems (biome 12), where it was positively correlated with species richness and diversity, and in deserts (biome 13) where it was negatively correlated with functional redundancy. MAP Risk was positively correlated with species richness across all biomes, and only in biome 12 and 13, negatively correlated with functional redundancy (Table 3).

Communities with low F_R and high MAT/MAP Risk are likely the most vulnerable to climate-driven changes in composition, as they face both, climate change–induced species turnover and a reduced capacity to maintain ecosystem function. These highly vulnerable sites are primarily located in the northern areas of the continent (Fig. 5). In contrast, communities with high F_R but high MAT/MAP Risk may still experience species loss but are expected to be more resilient in maintaining function; these are also concentrated in the continent's eastern interior. The least vulnerable communities—those with high F_R and low MAT/MAP Risk are scattered across central Australia (Fig. 5). The F_D–F_R ratio showed no association with temperature-driven risk (Spearman $\rho = -0.02$, $p = 0.56$), but was negatively associated with precipitation-driven risk ($\rho = -0.23$, $p \leq 0.001$), consistent with patterns observed for F_D and F_R separately

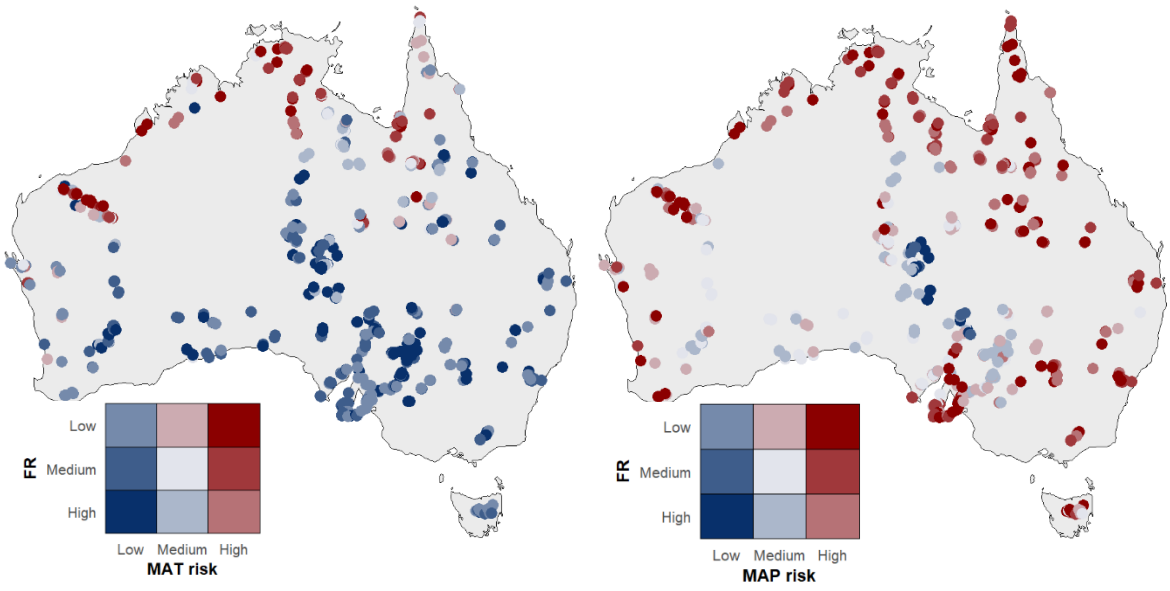

Figure 5. Bivariate maps of functional redundancy (F_R) and climate change risk across the Australian continent (646 TERN AusPlots). Left: F_R combined with mean annual temperature

risk (MAT Risk). Right: F_R combined with mean annual precipitation risk (MAP Risk). For F_R, plots were categorized using terciles (33rd and 67th percentiles), with mutually exclusive thresholds: low (bottom tercile), medium (second tercile), or high (top tercile). For MAT Risk, plots with risk < 0 were classified as low risk, whereas for MAP Risk, plots with risk > 0 were classified as low risk. Plots at risk (MAT risk ≥ 0 or MAP risk ≤ 0), were split into medium and high risk categories using the median of the at-risk subset. Plots with high climate risk and low F_R (dark red) are potentially most vulnerable to climate-driven changes in community composition and associated loss of ecosystem functionality.

Table 2. Best-fit linear models explaining variation in MAT Risk and MAP Risk against bioclimatic predictors across Australia and within selected biomes. Models were selected using AIC-based stepwise selection. The table reports the retained predictors, model fit statistics (adjusted R^2, sigma), and Akaike Information Criterion (AIC). The direction and statistical significance of each predictor in the best model are shown in brackets after each term (+: positive effect; –: negative effect; * $p \leq 0.05$, ** $p \leq 0.01$, *** $p \leq 0.001$). Predictors without brackets were retained in the best model but were not statistically significant.

Response Variable	Best model formula	Adj R^2	sigma	AIC	$df_{residual}$
MAT Risk	MAT Risk ~ 1 + $MAT^{(-*)}$ + $T\_Max^{(+***)}$ + $T\_Range^{(-***)}$ + $P\_Season^{(+***)}$	0.710	1.292	2372.09	701
MAP Risk	MAP Risk ~ 1 + $MAT^{(+***)}$ + $T\_Max^{(-***)}$ + $T\_Range^{(+***)}$ + $MAP^{(-***)}$ + $P\_Dry^{(-*)}$	0.879	94.066	8427.64	700
Biome 4 – Temperate broadleaf and mixed forests					
MAT Risk	MAT Risk ~ 1 + $MAT^{(+***)}$ + P_Dry	0.369	1.448	140.84	35
MAP Risk	MAP Risk ~ 1 + $MAT^{(-*)}$ + $T\_Max^{(+*)}$ + $T\_Range^{(-*)}$ + $MAP^{(+***)}$ + $P\_Dry^{(-*)}$	0.711	144.866	493.47	32
Biome 7 – Tropical / subtropical grasslands, savannas and shrublands					
MAT Risk	MAT Risk ~ 1 + $MAT^{(+***)}$ + $T\_Range^{(+***)}$ + $P\_Dry^{(+***)}$	0.758	0.692	413.93	190
MAP Risk	MAP Risk ~ 1 + MAT + $T\_Max^{(+***)}$ + $T\_Range^{(-***)}$ + $MAP^{(+***)}$ + $P\_Season^{(-***)}$	0.864	107.674	2373.95	188
Biome 12 – Mediterranean forests, woodlands and shrublands					
MAT Risk	MAT Risk ~ 1 + $T\_Max^{(+***)}$ + $P\_Season^{(+***)}$	0.264	1.570	704.44	184
MAP Risk	MAP Risk ~ 1 + $MAT^{(+***)}$ + $MAP^{(+***)}$ + $P\_Season^{(-***)}$	0.800	65.296	2099.56	183
Biome 13 – Deserts and xeric shrublands					
MAT Risk	MAT Risk ~ 1 + $MAT^{(+***)}$ + $T\_Max^{(+***)}$ + P-$Dry^{(-***)}$	0.767	0.940	673.78	242
MAP Risk	MAP Risk ~ 1 + $MAT^{(-***)}$ + $T\_Max^{(+***)}$ + $MAP^{(+***)}$ + P-$Dry^{(+***)}$	0.856	36.140	2470.07	241

Table 3. Direction and strength of pairwise relationships between climate change risk (MAT Risk and MAP Risk) and bioclimatic variables and diversity metrics (S_R = species richness, S_D = species diversity, F_D = functional diversity and F_R = functional redundancy) at the three spatial scales of study (i.e. continental Australia, and per biome). Values are Pearson correlation coefficients (r), which correspond to the direction of effects estimated in the simple linear regressions used for statistical testing. Positive r indicates variables increasing with climate risk; negative r indicates decreasing relationships. Significance codes: p ≤ 0.05 (*), ≤ 0.01 (**), ≤ 0.001 (***); n.s. = not significant.

	Diversity metrics			
	S_R	S_D	F_D	F_R
Continental Australia – all AusPlots				
MAT Risk	n.s.	n.s.	n.s.	n.s.
MAP Risk	0.41***	0.21***	0.21***	-0.08***
Biome 4 – Temperate broadleaf and mixed forests				
MAT Risk	n.s.	n.s.	n.s.	n.s.
MAP Risk	0.64***	n.s.	n.s	n.s.
Biome 7 – Tropical / subtropical grasslands, savannas and shrublands				
MAT Risk	n.s.	n.s.	n.s.	n.s.
MAP Risk	0.47***	0.34***	0.33***	n.s.
Biome 12 – Mediterranean forests, woodlands and shrublands				
MAT Risk	0.22**	0.20*	n.s.	n.s.
MAP Risk	0.44***	0.38*	0.23**	-0.25**
Biome 13 – Deserts and xeric shrublands				
MAT Risk	n.s.	n.s.	n.s.	-0.13*
MAP Risk	0.27***	0.18**	n.s.	-0.26***

4. Discussion

Here, we analysed multiple diversity metrics —including species richness, species diversity, functional diversity, and functional redundancy, but with particular emphasis on functional redundancy (F_R)— in Australian plant communities using continental-scale ecological and functional trait datasets. Functional redundancy is interpreted here as functional similarity, acknowledging that overlapping traits may buffer ecosystem functioning without implying full interchangeability among species or guaranteed resilience.

Our results showed that the northern Australian coastlines, are particularly vulnerable to species loss, shifts in community composition, and potential subsequent loss of ecosystem function due to future changes in temperature and precipitation. In addition, Mediterranean-climate regions in southwestern Western Australia and southeastern South Australia, are also vulnerable to precipitation-driven shifts in community composition.

We found that F_R was generally high across sampled communities and was positively associated with hot and increasingly arid environments, suggesting a greater potential for functional buffering in arid areas in the event of species loss (Walker 1995; Pimiento et al. 2020). (Walker 1995; Pimiento *et al.* 2020). Central arid plant communities may be functionally more resilient in the event of species loss given the structured pattern emerging of increasing F_R with distance from the coast.

At the continental scale, F_R variation was related to macroclimate in terms of both, temperature (MAT) and precipitation seasonality patterns (positive and negative relationships, respectively), while S_R, S_D and F_D showed opposite patterns (negative relationships with MAT and positive with MAP). However, these relationships explained limited variance, likely because macroclimate metrics do not capture fine-scale environmental variation, which can be a stronger driver of community composition. Declines in S_R with increasing temperature range suggest thermal variability acts as a filter, favouring stress-tolerant or generalist species, which could subsequently reduce F_D even if overall abundance is maintained.

Overall, the observed associations indicate that while F_R may contribute to buffering functional loss, this potential is context-dependent and often coincides with lower F_D, reflecting interactions between habitat filtering and niche partitioning (Spasojevic and Suding 2012). Together, these patterns underscore how functional traits and climatic variability combined shaping ecosystem resilience, and emphasise the need to understand how F_R and F_D respond to environmental gradients for conservation planning.

Andrew *et al.* (2021) found that F_D across Australian vegetation was strongly linked to climate using grid-cell-based models. In contrast, our plot-based analyses suggest communities

may possess greater F_R than broad-scale patterns would indicate, as local assembly processes—environmental filtering and biotic interactions—can enhance F_R, whereas grid-cell models reflect broader niche–environment relationships. Similarly, Guerin *et al.* (2022) found strong climate–trait links at the single-trait level across the same plot network, suggesting that aggregating traits into composite F_D and F_R metrics may dilute finer-scale trait–environment relationships. Although single trait studies can better reveal functional responses to environmental gradients (e.g., Funk *et al.* 2017), reductionist approaches offer more limited insights into community dynamics. Community assembly operates hierarchically, with macroclimate xerting broad constraints and local factors shaping communities at finer scales (Diaz et al. 1998; Laliberté et al. 2010). Consistent with this framework, we found that relationships between diversity metrics and climate were stronger when analysed within biomes than at the continental scale, particularly in Mediterranean systems (biome 12) and tropical/subtropical grasslands (biome 7). This may be related to greater floristic homogeneity and functional coherence within biomes compared to continental-scale analyses that integrate multiple species pools (Bruelheide *et al.* 2018).

At the biome scale, diversity metrics responded to bioclimate in highly context-specific ways, reflecting how climate interacts with physiology, resource availability, and evolutionary history to shape plant communities (Boonman *et al.* 2022). Contrasting responses of communities' F_R to bioclimatic factors within biomes indicate that different climatic stressors act as dominant constraints depending on biome-specific limiting factors. In tropical savannas (biome 7), strong rainfall seasonality limits species with narrow niches, while F_R increases with temperature range, likely reflecting convergence on heat-adapted strategies reported in seasonal tropical systems. Temperate forests (biome 4), characterised by relatively benign climatic conditions, show increasing species richness with warmth and species diversity with rainfall, whereas F_R remains largely independent of climate, consistent with weak environmental filtering. Mediterranean systems (biome 12) experience combined pressures of high temperatures and summer drought, leading to reduced S_R and S_D under hotter conditions, while F_R increases with reduced precipitation, likely driven by the dominance of stress-avoidance traits. Deserts (biome 13) show strong drought-driven F_R, although extreme heat constrains this response. In line with these patterns, we observed lower F_D at hotter and drier locations, and higher F_D at cooler and wetter locations. Climate-driven spatial patterns of functional diversity along contemporary climatic gradients have been reported previously (e.g. Guerin *et al.*, 2022), supporting our findings with regards to F_D. Nevertheless, our integrated analysis demonstrates that F_D alone is insufficient to understand ecosystem resilience, and that

the inclusion of F_R fundamentally alters the interpretation of climate–function relationships across biomes, and under future climate projections. Together, our results suggest that F_D-to-F_R ratio may reflect the interplay of habitat filtering, niche partitioning, and local environmental constraints (Kraft *et al.*, 2015), producing contrasting functional responses across biomes rather than reflecting climate alone. Consequently, communities with high F_D but low F_R may be more vulnerable to species loss, whereas communities with lower F_D but higher F_R may exhibit greater functional resilience (Ricotta *et al.* 2016).

Short-term drivers such as land-use change, disease, and direct anthropogenic pressures may further reduce F_R (Fonseca and Ganade 2001); however, our study focused on plant communities with minimal recent disturbance, suggesting that higher F_R under extreme environments reflects long-term environmental effects rather than human impact. We note, however, that because our analyses rely on contemporary surveys, current species composition may already incorporate recent climate- and land-use-driven shifts, which could influence trait filtering patterns and reduce predictive power. Inconsistent F_R metrics also complicate comparisons, emphasizing the need for clear methodology and fine-resolution environmental data when studying F_D and F_R (Biggs *et al.* 2020). Thus, we recommend clearly specifying F_R calculations and noting that functional similarity does not always imply redundancy, and we advocate for the use of finer-resolution environmental data (e.g., biome- or regional-scale) where available, to better elucidate F_D-to-F_R ratio and trends.

4.1. Climate change risk

Climate change risk exhibited clear geographic patterns across Australian plant communities and was strongly related to current climatic conditions, indicating that species safety margins may be more important than predicted exposure in determining the risk of species turnover or changes in community composition—a pattern that, while not previously demonstrated at the community level to the best of our knowledge, is consistent with species-level niche and tolerance theory (Araújo *et al.* 2013). Temperature-related risk (MAT Risk) varied with latitude, increasing from south to north, while precipitation-related risk (MAP Risk) was greatest in the coastline of the continent, especially in the North and in mediterranean-climate regions, and lowest at the arid centre. This, therefore, points to the northern coastline as a priority region for conservation practices to mitigate climate-driven change in vegetation communities.

In general, we found strong links between climate change risk and current climate conditions. The trends we found reflect the fact that as climates become more extreme in

762 temperature, species approach their tolerance limits, leading to the greatest temperature-driven
763 turnover in the hottest and most seasonally variable environments (Deutsch et al. 2008), a
764 pattern consistent with climate-driven vulnerability contrasts reported for European plant
765 communities (Thuiller *et al.* 2005). For example, MAT Risk increased with long-term T-max
766 and P-Season and decreased with MAT and T-Range, suggesting that communities exposed to
767 persistently high temperature extremes and strong intra-annual rainfall variability will be most
768 sensitive to future warming, whereas broader thermal ranges may buffer against turnover. In
769 contrast, MAP Risk was highest in sites experiencing pronounced temperature fluctuations, but
770 lowest in sites with high rainfall and dry-season precipitation, implying that plant communities
771 subjected to the combined pressures of heat and drought will face higher precipitation-driven
772 risk. Together, these patterns suggest that climatic safety margins may be more important than
773 predicted exposure *per se* in determining sensitivity to climate change in Australian plant
774 communities (Foden *et al.* 2019), as safety margins span a wider range of values than projected
775 exposure across the continent. We acknowledge that species' climate tolerances are derived
776 from their realised rather than fundamental niches, potentially underestimating true
777 physiological limits and adaptive capacity (Sax *et al.* 2013). Yet, species already persisting in
778 extreme environments may possess greater adaptive potential precisely because of being
779 shaped by harsher conditions (Chevin and Hoffmann 2017).

780 At the biome scale, the links between climatic variables and MAT and MAP Risk
781 highlight how different vegetation types may be exposed to shifts in community composition
782 under warming and drying trends. The benign climatic conditions of temperate forests (biome
783 4) make them vulnerable to temperature stress (i.e. increases in MAT and T-Max positively
784 affect MAT and MAP Risk respectively) and rainfall (i.e. lower P-Dry results in higher MAP
785 Risk), reflecting their dependence on stable mild temperatures and moisture regimes.

786 Tropical savannas in northern Australia, where MAT Risk was found to be highest, are
787 key global carbon sinks (Grace *et al.* 2006) that rely on complex interactions between fire
788 regimes, water availability and vegetation dynamics (Moore *et al.* 2018), making them highly
789 vulnerable to climatic shifts (Lehman *et al.* 2011). MAT Risk increased in hotter sites and in
790 areas with greater dry-season rainfall, indicating that both chronic warmth and large annual
791 temperature fluctuations amplify sensitivity to warming. MAP Risk, by contrast, was highest
792 in wetter and more heat-exposed savannas but declined with greater temperature range and
793 rainfall seasonality, suggesting that climatic variability and pronounced wet–dry cycles may
794 help buffer these communities against precipitation-driven change. Their high sensitivity to
795 future precipitation shifts (MAP Risk) likely stem from the fact that these ecosystems are

structured around strong wet–dry seasonality, where even small changes in rainfall amount or timing can disrupt plant recruitment, survival, and competitive ability (Murphy and Bowman 2012). Unlike species in more southern arid zones, many northern taxa are less drought-adapted, thus, reduced rainfall could push them beyond their physiological limits (Foden *et al.* 2019). Moreover, biogeographic barriers constrain range shifts, as deserts to the south and oceans to the north limit gradual migration. Together, these factors indicate that northern Australia warrants particular attention from land managers and conservation purposes to prevent climate-driven species loss.

Mediterranean regions in the South West Australian Floristic Region (SWAFR) and South Australia showed high MAP Risk probably due to many species in these communities already nearing their upper climate thresholds, particularly with regards to the intense summer drought periods they face (Lewandrowski *et al.* 2021). In fact, drought-related dieback of Australian mediterranean vegetation has been well-documented, with rainfall already in decline and predicted to continue (Brouwers *et al.* 2013). Both MAT and MAP Risk were highest in the warmest areas and in sites with weaker rainfall seasonality, indicating that communities occupying the margins of the Mediterranean climate regime —where summer drought is less pronounced— are more vulnerable to climate-driven change than those in strongly seasonal, drought-adapted environments, pointing to the importance of stress-tolerant adaptations in buffering these communities against increasing drought.

Deserts and arid interiors exhibited low MAP Risk, due to projected increases in precipitation by 2070 (Gallagher *et al.* 2019), reflecting reduced drought stress within the bounds of the MAP Risk metric. Importantly, the MAP Risk metric used here is designed to capture risk associated with increasing drought stress and does not explicitly account for potential negative effects of increased precipitation (e.g. moisture intolerance or competitive displacement of arid-adapted species) in arid communities. MAT Risk was greatest in the hottest sites and declined with P-Dry, indicating that hyper-arid communities already adapted to extreme water limitation may be less sensitive to further warming than those in comparatively milder desert environments. MAP Risk, however, increased in warmer and wetter desert areas and in sites where the driest month is less dry, suggesting that communities located in more semi-arid areas are more vulnerable to precipitation-driven change than those in the most extremely water-limited regions that are already adapted to drought.

Together, these contrasting biome-level responses indicate that climate-change risk is shaped not only by absolute climatic stress but by how far future conditions will diverge from the specific adaptive strategies of the vegetation characteristic of each biome, thus underscoring

the need for case-by-case assessments and the challenge of making generalizations when predicting changes in vegetation dynamics (Mori 2011). Although we focused on mean climate changes, we acknowledge that extreme events (e.g. heatwaves, droughts and wildfires) can also shape species survival and drive ecosystem shifts (Lloret *et al.* 2012).

4.2. Relationship between functional redundancy and climate change risk

By integrating climate change risk with F_R, we provide a robust assessment of Australian plant communities, capturing both their vulnerability to species loss and their potential resilience to functional disruption (traditionally ignored in climate change studies; Li *et al.* 2018). Within this framework, communities experiencing high climate risk and low F_R are expected to be most vulnerable to functional destabilisation, whereas communities facing high risk but with high F_R may buffer some functional loss (Walker 1992, 1995; Ricotta *et al.* 2016). Communities exposed to low climate risk are, by contrast, inherently less threatened.

At the national scale, unlike MAT Risk, MAP Risk showed significant correlations with all biodiversity metrics, reflecting the strong influence of rainfall and its seasonality on Australian flora, pointing the northern coastline as well as the mediterranean-climate regions as the most vulnerable areas to suffer changes in community composition and subsequent loss of ecosystem function. The significant association between precipitation-driven risk and the F_D–F_R ratio indicates that changes in rainfall disproportionately affect communities where functional similarity is high relative to functional diversity, increasing the likelihood of coordinated species responses rather than compensatory dynamics. Biome-level patterns suggested that functional traits, rather than species richness *per se*, determine resilience, with vulnerability arising from the loss of overlapping functions that stabilize vegetation communities against climate-driven changes.

At the biome scale, the influence of community diversity on climate-change risk varied markedly. Across all biomes, communities with larger species pools tended to experience stronger compositional shifts under warming and altered rainfall, perhaps reflecting the exposure of less stress-tolerant species. Whereas no significant trends were found between functional redundancy and climate-driven changes in temperate forest (biome 4) and tropical savannas (biome 7), F_R covaried with precipitation-driven risk in arid ecosystems, with desert and Mediterranean biomes exhibiting high F_R associated with MAP Risk, consistent with redundancy in stress-tolerant traits that may buffer against future drought conditions. In Mediterranean vegetation communities (biome 12), higher functional redundancy was associated with lower precipitation-driven risk, highlighting the role of overlapping functional

traits in stabilising communities despite turnover in species composition. In deserts (biome 13), contrasting relationships between species diversity, functional diversity, and climate-driven risk indicate that vulnerability in arid communities reflects a balance between the breadth of functional strategies and species identities, with some aspects of diversity associated with greater turnover and others with enhanced resilience. Altogether, these patterns indicate that precipitation-driven climate risk shows stronger associations with community structure than temperature-driven risk, and that the ecological consequences of diversity for climate vulnerability are highly context-dependent, reflecting the specific adaptive strategies and functional composition of each biome.

4.3. Applications and future directions

Functional redundancy is most often conceptualised in relation to species loss; however, climate change is also expected to drive species gains, with newly arriving species exerting a wide range of functional effects. These effects may enhance community resilience, for example by supporting mutualistic interactions, or conversely disrupt ecosystem functioning, particularly when incoming species are non-native or competitively dominant (Traveset *et al.* 2013; Wardle *et al.* 2011). Accurately predicting climate-driven community responses therefore requires accounting for both species loss and species gain, rather than focusing on extinction processes alone (Gallagher *et al.* 2013).

Ideally, functional redundancy would be quantified using effect traits explicitly linked to ecosystem functions and response traits linked to specific environmental stressors; however, this distinction is often difficult to implement because traits can act as either depending on context (Suding *et al.* 2008). At continental scales, these challenges are compounded by limitations in trait availability, underscoring the importance of large open-access trait databases such as AusTraits and continued efforts to improve taxonomic coverage (Falster *et al.* 2021). Consequently, large-scale studies commonly assume that higher functional redundancy captures at least some degree of response diversity (Laliberté *et al.* 2010; Pillar *et al.* 2013).

Within these constraints, our results provide a continent-wide framework linking functional redundancy with climate-driven risk in Australian plant communities, with clear relevance for conservation planning and land management (Walker 1995; Rosenfeld 2002). In particular, prioritising communities identified as both highly exposed to climate change and functionally vulnerable—such as those in the tropical North and Mediterranean regions—may help safeguard key ecosystem functions. Maintaining communities with high functional redundancy may contribute to buffering ecosystem functioning under ongoing environmental

change (Mori *et al.* 2013), while recognising that redundancy does not guarantee resilience.

Future research should explicitly test whether the spatial patterns of functional redundancy identified here translate into realised ecosystem resilience through time, particularly following repeated or extreme climatic disturbances (Biggs *et al.* 2020). Long-term, standardised monitoring networks such as TERN AusPlots, combined with trait-based data from AusTraits, provide a robust foundation for evaluating when and where functional buffering persists or fails, thereby refining predictions of climate-driven ecosystem vulnerability and supporting more targeted conservation strategies.

5. Conclusions

Australian plant communities show strong regional variation in vulnerability to climate change, with the tropical north being at greatest risk due to shifts in rainfall and temperature combined with low functional redundancy, followed by the mediterranean regions of Western and South Australia. Across the continent, areas characterised by high projected climate-driven compositional change and low functional redundancy represent communities with the lowest potential buffering capacity against functional loss or disruption. These findings highlight priority areas for monitoring and management, providing a framework to safeguard ecosystem function under a changing climate. Targeted monitoring and prioritizing proactive management in these hotspots of high at-risk vegetation communities is therefore critical to prevent irreversible functional loss under future climate scenarios.

Author Contributions

I.M.-F. and G.R.G. had the initial idea for the paper. R.V.M., I.M.-F., and S.C.A. contributed to data analysis; I.M.-F. and R.V.M. produced results and figures with recommendations from other authors. All authors contributed to drafting the paper, reviewed the manuscript and gave final approval for publication.

Acknowledgements

The AusTraits project received investment (https://doi.org/10.47486/TD044, https://doi.org/10.47486/DP720) from the Australian Research Data Commons (ARDC). The ARDC is funded by the National Collaborative Research Infrastructure Strategy (NCRIS). This work is supported by the use of Terrestrial Ecosystem Research Network (TERN) infrastructure, which is enabled by the Australian Government's National Collaborative Research Infrastructure Strategy (NCRIS).

References

Ackerly, DD, Cornwell, WK (2007) A trait-based approach to community assembly: partitioning of species trait values into within-and among-community components. *Ecology Letters* **10**, 135-145.

Aguirre-Gutiérrez, J, Berenguer, E, Oliveras Menor, I, Bauman, D, Corral-Rivas, JJ, Nava-Miranda, MG, Both, S, Ndong, JE, Ondo, FE, Bengone, NNs, Mihinhou, V, Dalling, JW, Heineman, K, Figueiredo, A, González-M, R, Norden, N, Hurtado-M, AB, González, D, Salgado-Negret, B, Reis, SM, Moraes de Seixas, MM, Farfan-Rios, W, Shenkin, A, Riutta, T, Girardin, CAJ, Moore, S, Abernethy, K, Asner, GP, Bentley, LP, Burslem, DFRP, Cernusak, LA, Enquist, BJ, Ewers, RM, Ferreira, J, Jeffery, KJ, Joly, CA, Marimon-Junior, BH, Martin, RE, Morandi, PS, Phillips, OL, Bennett, AC, Lewis, SL, Quesada, CA, Marimon, BS, Kissling, WD, Silman, M, Teh, YA, White, LJT, Salinas, N, Coomes, DA, Barlow, J, Adu-Bredu, S, Malhi, Y (2022) Functional susceptibility of tropical forests to climate change. *Nature Ecology and Evolution* **6**, 878-889.

Andrew, SC, Mokany, K, Falster, DS, Wenk, E, Wright, IJ, Merow, C, Adams, V, Gallagher, RV (2021) Functional diversity of the Australian flora: strong links to species richness and climate. *Journal of Vegetation Science* **32**, e13018.

Andrew, SC, Martín-Forés, I, Guerin, G, Coleman, D, Falster, D, Wenk, E, Wright, I, Gallagher, RV (2025) Mapping plant functional traits using gap-filled datasets to inform management and modelling. *Global Ecology and Biogeography* **34**, e70136.

Aphalo, P (2025) ggpmisc: Miscellaneous Extensions to 'ggplot2'.

Araújo, MB, Ferri-Yáñez, F, Bozinovic, F, Marquet, PA, Valladares, F, Chown, SL (2013) Heat freezes niche evolution. *Ecology Letters* **16**, 1206-1219.

Bailey, HP (1964) Toward a unified concept of the temperate climate. *Geographical Review* **54**, 516-545.

Bates, DM (2010) lme4: Mixed-effects modeling with R. Springer New York,

Bennett, JM, Sunday, J, Calosi, P, Villalobos, F, Martínez, B, Molina-Venegas, R, Araújo, MB, Algar, AC, Clusella-Trullas, S, Hawkins, BA, Keith, SA, Kühn, I, Rahbek, C, Rodríguez, L, Singer, A, Morales-Castilla, I, Olalla-Tárraga, MÁ (2021) The evolution of critical thermal limits of life on Earth. *Nature communications*, **12**, 1198.

Biggs, CR, Yeager, LA, Bolser, DG, Bonsell, C, Dichiera, AM, Hou, Z, Keyser, SR, Khursigara, AJ, Lu, K, Muth, AF (2020) Does functional redundancy affect

ecological stability and resilience? A review and meta-analysis. *Ecosphere* **11**, e03184.

Boonman, CC, Huijbregts, MA, Benítez-López, A, Schipper, AM, Thuiller, W, Santini, L (2022) Trait-based projections of climate change effects on global biome distributions. *Diversity and Distributions*, **28**, 25-37.

Borgy, B, Violle, C, Choler, P, Garnier, E, Kattge, J, Loranger, J, Amiaud, B, Cellier, P, Debarros, G, Denelle, P (2017) Sensitivity of community-level trait–environment relationships to data representativeness: A test for functional biogeography. *Global Ecology and Biogeography* **26**, 729-739.

Botta-Dukát, Z (2005) Rao's quadratic entropy as a measure of functional diversity based on multiple traits. *Journal of Vegetation Science* **16**, 533-540.

Brouwers, NC, Mercer, J, Lyons, T, Poot, P, Veneklaas, E, Hardy, G (2013) Climate and landscape drivers of tree decline in a Mediterranean ecoregion. *Ecology and Evolution* **3**, 67-79.

Bruelheide, H, Dengler, J, Purschke, O, Lenoir, J, Jiménez-Alfaro, B, Hennekens, SM, Botta-Dukát, Z, Chytrý, M, Field, R, Jansen, F, Kattge, J, Pillar, VD, Schrodt, F, Mahecha, MD, Peet, RK, Sandel, B, van Bodegom, P, Altman, J, Alvarez-Dávila, E, Arfin Khan, MAS, Attorre, F, Aubin, I, Baraloto, C, Barroso, JG, Bauters, M, Bergmeier, E, Biurrun, I, Bjorkman, AD, Blonder, B, Čarni, A, Cayuela, L, Černý, T, Cornelissen, JHC, Craven, D, Dainese, M, Derroire, G, De Sanctis, M, Díaz, S, Doležal, J, Farfan-Rios, W, Feldpausch, TR, Fenton, NJ, Garnier, E, Guerin, GR, Gutiérrez, AG, Haider, S, Hattab, T, Henry, G, Hérault, B, Higuchi, P, Hölzel, N, Homeier, J, Jentsch, A, Jürgens, N, Kącki, Z, Karger, DN, Kessler, M, Kleyer, M, Knollová, I, Korolyuk, AY, Kühn, I, Laughlin, DC, Lens, F, Loos, J, Louault, F, Lyubenova, MI, Malhi, Y, Marcenò, C, Mencuccini, M, Müller, JV, Munzinger, J, Myers-Smith, IH, Neill, DA, Niinemets, Ü, Orwin, KH, Ozinga, WA, Penuelas, J, Pérez-Haase, A, Petřík, P, Phillips, OL, Pärtel, M, Reich, PB, Römermann, C, Rodrigues, AV, Sabatini, FM, Sardans, J, Schmidt, M, Seidler, G, Silva Espejo, JE, Silveira, M, Smyth, A, Sporbert, M, Svenning, J-C, Tang, Z, Thomas, R, Tsiripidis, I, Vassilev, K, Violle, C, Virtanen, R, Weiher, E*et al.* (2018) Global trait–environment relationships of plant communities. *Nature Ecology and Evolution* **2**, 1906-1917.

Cadotte, MW, Carscadden, K, Mirotchnick, N (2011) Beyond species: functional diversity and the maintenance of ecological processes and services. *Journal of applied ecology* **48**, 1079-1087.

Chevin, LM, Hoffmann, AA (2017) Evolution of phenotypic plasticity in extreme environments. *Philosophical Transactions of the Royal Society B: Biological Sciences* **372**, 20160138.

Deutsch, CA, Tewksbury, JJ, Huey, RB, Sheldon, KS, Ghalambor, CK, Haak, DC, Martin, PR (2008) Impacts of climate warming on terrestrial ectotherms across latitude. *Proceedings of the National Academy of Sciences* **105**, 6668-6672.

Díaz, S, Kattge, J, Cornelissen, JH, Wright, IJ, Lavorel, S, Dray, S, Reu, B, Kleyer, M, Wirth, C, Colin Prentice, I (2016) The global spectrum of plant form and function. *Nature* **529**, 167-171.

Díaz, S, Settele, J, Brondízio ES, Ngo, HT, Guèze, M, Agard, J, Arneth, A, Balvanera, P, Brauman, KA, Butchart, SHM, Chan, KMA, Garibaldi, LA, Ichii, K, Liu, J, Subramanian, SM, Midgley, GF, Miloslavich, P, Molnár, Z, Obura, D, Pfaff, A, Polasky, S, Purvis, A, Razzaque, J, Reyers, B, Roy Chowdhury, R, Shin, YJ, Visseren-Hamakers, IJ, Willis, KJ, Zayas, CN (Eds.) IPBES (2019): Summary for policymakers of the global assessment report on biodiversity and ecosystem services of the Intergovernmental Science-Policy Platform on Biodiversity and Ecosystem Services. IPBES secretariat, Bonn, Germany. 56 pages.

Di Marco, M, Harwood, TD, Hoskins, AJ, Ware, C, Hill, SL, Ferrier, S (2019) Projecting impacts of global climate and land-use scenarios on plant biodiversity using compositional-turnover modelling. *Global Change Biology* **25**, 2763-2778

Elmqvist, T, Folke, C, Nyström, M, Peterson, G, Bengtsson, J, Walker, B, Norberg, J (2003) Response diversity, ecosystem change, and resilience. *Frontiers in Ecology and the Environment* **1**, 488-494.

Eisenhäuer, N, Hines, J, Maestre, FT, Rillig, MC (2023). Reconsidering functional redundancy in biodiversity research. *npj Biodiversity* **2**, 9.

Falster, D. S., & Westoby, M. (2003). Plant height and evolutionary games. *Trends in Ecology and Evolution*, **18**, 337-343.

Falster, D, Gallagher, R, Wenk, EH, Wright, IJ, Indiarto, D, Andrew, SC, Baxter, C, Lawson, J, Allen, S, Fuchs, A (2021) AusTraits, a curated plant trait database for the Australian flora. *Scientific data* **8**, 1-20.

Fick, SE, Hijmans, RJ (2017) WorldClim 2: new 1-km spatial resolution climate surfaces for global land areas. *International journal of climatology* **37**, 4302-4315.

Fischer, FM, de Bello, F (2023) On the uniqueness of functional redundancy. *npj Biodiversity* **2**, 23.

1033 Foden, WB, Young, BE, Akçakaya, HR, Garcia, RA, Hoffmann, AA, Stein, BA, Thomas,
1034 CD, Wheatley, CJ, Bickford, D, Carr, JA, Hole, DG, Martin, TG, Pacifici, M, Pearce-
1035 Higgins, JW, Platts, PJ, Visconti, P, Watson, JEM, Huntley, B (2019) Climate change
1036 vulnerability assessment of species. *Wiley Interdisciplinary Reviews: Climate*
1037 *Change* **10**, e551.
1038 Fonseca, CR, Ganade, G (2001) Species functional redundancy, random extinctions and the
1039 stability of ecosystems. *Journal of Ecology* **89**, 118-125.
1040 Funk, JL, Larson, JE, Ames, GM, Butterfield, BJ, Cavender-Bares, J, Firn, J, Laughlin, DC,
1041 Sutton-Grier, AE, Williams, L, Wright, J (2017) Revisiting the H oly G rail: using
1042 plant functional traits to understand ecological processes. *Biological reviews* **92**,
1043 1156-1173.
1044 Gallagher, RV, Allen, S, Wright, IJ (2019) Safety margins and adaptive capacity of
1045 vegetation to climate change. *Scientific Reports* **9**, 1-11.
1046 Gallagher, RV, Hughes, L, Leishman, MR (2013) Species loss and gain in communities
1047 under future climate change: consequences for functional diversity. *Ecography* **36**,
1048 531-540.
1049 Gallagher, RV, Falster, DS, Maitner, BS, Salguero-Gómez, R, Vandvik, V, Pearse, WD,
1050 Schneider, FD, Kattge, J, Poelen, JH, Madin, JS, Ankenbrand, MJ, Penone, C, Feng,
1051 X, Adams, VM, Alroy, J, Andrew, SC, Balk, MA, Bland, LM, Boyle, BL, Bravo-
1052 Avila, CH, Brennan, I, Carthey, AJR, Catullo, R, Cavazos, BR, Conde, DA, Chown,
1053 SL, Fadrique, B, Gibb, H, Halbritter, AH, Hammock, J, Hogan, JA, Holewa, H, Hope,
1054 M, Iversen, CM, Jochum, M, Kearney, M, Keller, A, Mabee, P, Manning, P,
1055 McCormack, L, Michaletz, ST, Park, DS, Perez, TM, Pineda-Munoz, S, Ray, CA,
1056 Rossetto, M, Sauquet, H, Sparrow, B, Spasojevic, MJ, Telford, RJ, Tobias, JA, Violle,
1057 C, Walls, R, Weiss, KCB, Westoby, M, Wright, IJ, Enquist, BJ (2020) Open Science
1058 principles for accelerating trait-based science across the Tree of Life. *Nature Ecology*
1059 *and Evolution* **4**, 294-303.
1060 Grace, J, José, JS, Meir, P, Miranda, HS, Montes, RA (2006) Productivity and carbon fluxes
1061 of tropical savannas. *Journal of Biogeography* **33**, 387-400.
1062 Guerin, GR, Gallagher, RV, Wright, IJ, Andrew, SC, Falster, DS, Wenk, E, Munroe, SEM,
1063 Lowe, AJ, Sparrow, B (2022) Environmental associations of abundance-weighted
1064 functional traits in Australian plant communities. *Basic and Applied Ecology* **58**, 98-
1065 109.

1066 Guerin, GR, Williams, KJ, Sparrow, B, Lowe, AJ (2020a) Stocktaking the environmental
1067 coverage of a continental ecosystem observation network. *Ecosphere* **11**, e03307.
1068 Guerin, G, Saleeba, T, Munroe, S, Blanco-Martin, B, Martín-Forés, I, Tokmakoff, A (2020b)
1069 ausplotsR: TERN AusPlots analysis package. *R package version* **1**,
1070 Hooper, DU, Adair, EC, Cardinale, BJ, Byrnes, JEK, Hungate, BA, Matulich, KL, Gonzalez,
1071 A, Duffy, JE, Gamfeldt, L, O'Connor, MI (2012) A global synthesis reveals
1072 biodiversity loss as a major driver of ecosystem change. *Nature* **486**, 105-108.
1073 Hughes, L (2003) Climate change and Australia: trends, projections and impacts. *Austral*
1074 *Ecology* **28**, 423-443.
1075 Keith, DA (Ed.) (2017) Australian vegetation. Cambridge University Press.
1076 Kraft, NJ, Adler, PB, Godoy, O, James, EC, Fuller, S, Levine, JM (2015) Community
1077 assembly, coexistence and the environmental filtering metaphor. *Functional*
1078 *Ecology* **29**, 592-599.
1079 Laliberté E, Wells, JA, DeClerck, F, Metcalfe, DJ, Catterall, CP, Queiroz, C, Aubin, I,
1080 Bonser, SP, Ding, Y, Fraterrigo, JM (2010) Land-use intensification reduces
1081 functional redundancy and response diversity in plant communities. *Ecology Letters*
1082 **13**, 76-86.
1083 Lancaster, LT, Humphreys, AM (2020) Global variation in the thermal tolerances of
1084 plants. *Proceedings of the National Academy of Sciences* **117**, 13580-13587.
1085 Lehmann, CE, Archibald, SA, Hoffmann, WA, Bond, WJ (2011) Deciphering the distribution
1086 of the savanna biome. *New Phytologist* **191**, 197-209.
1087 Lewandrowski, W, Stevens, JC, Webber, BL, L. Dalziell, E, Trudgen, MS, Bateman, AM,
1088 Erickson, TE (2021) Global change impacts on arid zone ecosystems: Seedling
1089 establishment processes are threatened by temperature and water stress. *Ecology and*
1090 *Evolution* **11**, 8071-8084.
1091 Li, D, Wu, S, Liu, L, Zhang, Y, Li, S (2018) Vulnerability of the global terrestrial ecosystems
1092 to climate change. *Global change biology* **24**, 4095-4106.
1093 Lionello, P, Malanotte-Rizzoli, P, Boscolo, R, Alpert, P, Artale, V, Li, L, Luterbacher, J,
1094 May, W, Trigo, R, Tsimplis, M, Ulbrich, U, Xoplaki, E (2006) The Mediterranean climate:
1095 an overview of the main characteristics and issues. *Developments in Earth and*
1096 *Environmental Sciences* **4**, 1-26.
1097 Lloret, F, Escudero, A, Iriondo, JM, Martínez-Vilalta, J, Valladares, F (2012) Extreme
1098 climatic events and vegetation: the role of stabilizing processes. *Global change*
1099 *biology* **18**, 797-805.

1100 Moore, CE, Beringer, J, Donohue, RJ, Evans, B, Exbrayat, J-F, Hutley, LB, Tapper, NJ
1101 (2018) Seasonal, interannual and decadal drivers of tree and grass productivity in an
1102 Australian tropical savanna. *Global change biology* **24**, 2530-2544.
1103 Mori, AS (2011) Ecosystem management based on natural disturbances: hierarchical context
1104 and non-equilibrium paradigm. *Journal of applied ecology* **48**, 280-292.
1105 Mori, AS, Furukawa, T, Sasaki, T (2013) Response diversity determines the resilience of
1106 ecosystems to environmental change. *Biological reviews* **88**, 349-364.
1107 Mouillot, D, Graham, NA, Villéger, S, Mason, NW, Bellwood, DR (2013). A functional
1108 approach reveals community responses to disturbances. *Trends in ecology and*
1109 *evolution* **28**, 167-177.
1110 Munroe, S, Guerin, G, Saleeba, T, Martín-Forés, I, Blanco-Martin, B, Sparrow, B,
1111 Tokmakoff, A (2021) ausplotsR: An R package for rapid extraction and analysis of
1112 vegetation and soil data collected by Australia's Terrestrial Ecosystem Research
1113 Network. *Journal of Vegetation Science* **32**, e13046
1114 Murphy, BP, Bowman, DM (2012) What controls the distribution of tropical forest and
1115 savanna?. *Ecology Letters* **15**, 748-758.
1116 Noy-Meir, I (1973) Desert ecosystems: environment and producers. *Annual review of ecology*
1117 *and systematics* **4**, 25-51.
1118 Olson, DM, Dinerstein, E, Wikramanayake, ED, Burgess, ND, Powell, GVN, Underwood,
1119 EC, D'amico, JA, Itoua, I, Strand, HE, Morrison, JC, Loucks, CJ, Allnutt, TF,
1120 Ricketts, TH, Kura, Y, Lamoreux, JF, Wettengel, WW, Hedao, P, Kassem, KR (2001)
1121 Terrestrial Ecoregions of the World: A New Map of Life on Earth: A new global map
1122 of terrestrial ecoregions provides an innovative tool for conserving biodiversity.
1123 *BioScience* **51**, 933-938.
1124 Pettorelli, N, Graham, NA, Seddon, N, da Cunha Bustamante, M, Lowton, MJ, Sutherland,
1125 WJ, Koldwey, HJ, Prentice, HC, Barlow, J (2021) Time to integrate global climate
1126 change and biodiversity science-policy agendas. *Journal of Applied Ecology* **58**,
1127 2384-2393.
1128 Pillar, VD, Blanco, CC, Müller, SC, Sosinski, EE, Joner, F, Duarte, LD (2013) Functional
1129 redundancy and stability in plant communities. *Journal of Vegetation Science* **24**,
1130 963-974.
1131 Pimiento, C, Bacon, CD, Silvestro, D, Hendy, A, Jaramillo, C, Zizka, A, Meyer, X,
1132 Antonelli, A (2020) Selective extinction against redundant species buffers functional
1133 diversity. *Proceedings of the Royal Society B* **287**, 20201162.

RCoreTeam (2018) The R Stats Package *CRAN Repository, R*

Ricotta, C, de Bello, F, Moretti, M, Caccianiga, M, Cerabolini, BE, Pavoine, S (2016) Measuring the functional redundancy of biological communities: a quantitative guide *Methods in Ecology and Evolution* **7**, 1386-1395

Rosenfeld, JS (2002) Functional redundancy in ecology and conservation. *Oikos* **98**, 156-162.

Sax, DF, Early, R, Bellemare, J (2013) Niche syndromes, species extinction risks, and management under climate change. *Trends in Ecology and Evolution* **28**, 517-523.

Schrodt, F, Kattge, J, Shan, H, Fazayeli, F, Joswig, J, Banerjee, A, Reichstein, M, Bönisch, G, Díaz, S, Dickie, J, Gillison, A, Karpatne, A, Lavorel, S, Leadley, P, Wirth, JC, Wright, IJ, Wright, SJ, Reich, P.B (2015) BHPMF–a hierarchical Bayesian approach to gap-filling and trait prediction for macroecology and functional biogeography. *Global Ecology and Biogeography* **24**, 1510-1521.

Shaw, RB, Jacobs, SWL, Everett, J (2000) Tropical grasslands and savannas. Grasses: Systematics and Evolution. CSIRO, Melbourne: CSIRO, 351-355.

Sparrow, BD, Foulkes, JN, Wardle, GM, Leitch, EJ, Caddy-Retalic, S, Van Leeuwen, SJ, Tokmakoff, A, Thurgate, NY, Guerin, GR, Lowe, AJ (2020) A vegetation and soil survey method for surveillance monitoring of rangeland environments. *Frontiers in Ecology and Evolution* **8**, 157.

Spasojevic, MJ, Suding, KN (2012) Inferring community assembly mechanisms from functional diversity patterns: the importance of multiple assembly processes. *Journal of Ecology* **100**, 652-661.

State of the Climate 2024, CSIRO and Bureau of Meteorology, © Government of Australia.

Suding, KN, Lavorel, S, Chapin Iii, F, Cornelissen, JH, Díaz, S, Garnier, E, Goldberg, D, Hooper, DU, Jackson, ST, Navas, ML (2008) Scaling environmental change through the community-level: A trait-based response-and-effect framework for plants. *Global change biology* **14**, 1125-1140.

Traveset, A, Heleno, R, Chamorro, S, Vargas, P, McMullen, CK, Castro-Urgal, R, Nogales, M, Herrera, HW, Olesen, JM (2013) Invaders of pollination networks in the Galápagos Islands: emergence of novel communities. *Proceedings of the Royal Society B: Biological Sciences* **280**, 20123040.

Thuiller, W, Lavorel, S, Araújo, MB, Sykes, MT, Prentice, IC (2005) Climate change threats to plant diversity in Europe. *Proceedings of the National Academy of Sciences* **102**, 8245-8250.

1167 Valladares, F, Magro, S, Martín-Forés, I (2019). Anthropocene, the challenge for *Homo*
1168 *sapiens* to set its own limits. *Cuadernos de Investigación Geográfica*, **45**, 33-59.
1169 Violle, C, Reich, PB, Pacala, SW, Enquist, BJ, Kattge, J (2014) The emergence and promise
1170 of functional biogeography. *Proceedings of the National Academy of Sciences* **111**,
1171 13690-13696.
1172 Walker, B (1992) Biodiversity and ecological redundancy. *Conservation Biology* **6**, 18–23.
1173 Walker, B (1995) Conserving biological diversity through ecosystem resilience.
1174 *Conservation Biology* **9**, 747-752.
1175 Wardle, DA, Bardgett, RD, Callaway, RM, Van der Putten, WH (2011) Terrestrial ecosystem
1176 responses to species gains and losses. *Science* **332**, 1273-1277.
1177 Westoby, M (1998) A leaf-height-seed (LHS) plant ecology strategy scheme. *Plant and soil*
1178 **199**, 213-227.
1179 White, A, Sparrow, B, Leitch, E, Foulkes, J, Flitton, R, Lowe, AJ, Caddy-Retalic, S (2012)
1180 AUSPLOTS rangelands survey protocols manual.
1181 Wickham, H (2016) ggplot2: Elegant Graphics for Data Analysis. Springer-Verlag New
1182 York.
1183 Wright, IJ, Reich, PB, Westoby, M, Ackerly, DD, Baruch, Z, Bongers, F, Cavender-Bares, J,
1184 Chapin, T, Cornelissen, JH, Diemer, M (2004) The worldwide leaf economics
1185 spectrum. *Nature* **428**, 821-827.